Application of a Regression-Based EOS PVT Program to Laboratory Data

K.H. Coats, SPE, Scientific Software-Intercomp
G.T. Smart,* SPE, Scientific Software-Intercomp

SPE 11197

Summary. An equation-of-state (EOS)-based PVT program was applied to match laboratory PVT data for three published and nine additional reservoir fluid samples. This paper includes laboratory test data for the nine samples and describes PVT program features, especially regression, that we find conducive to rapid determination of EOS parameter values needed to match data. With regression, both the Peng-Robinson (PR) and Zudkevitch-Joffe-Redlich-Kwong (ZJRK) EOS give comparable and generally good agreement with laboratory data. Without regression or significant adjustment of EOS parameters, neither EOS adequately predicts observed reservoir fluid PVT behavior.

Our EOS tuning uses a small degree of C_{7+} fraction splitting. The agreement of these EOS results with data compares favorably with that obtained in previously published studies that used extensive C_{7+} splitting.

Introduction

A recent trend in compositional simulation is the use of an EOS, as opposed to independent correlations, to calculate K-values and equilibrium-phase properties. An important prerequisite in meaningful use of the EOS-based compositional model is satisfactory agreement between EOS results and laboratory PVT test data relevant to the reservoir fluid and recovery process.

A number of studies[1-9] report comparisons of cubic EOS and laboratory PVT results for a wide variety of reservoir fluids and conditions. Most of these studies emphasize the C_{7+} characterization as the key element in attaining agreement between EOS and laboratory results. Some studies use more than 40 components that result from splitting the C_{7+} fraction. Some authors imply a predictive EOS capability provided one EOS parameter is adjusted to match the reservoir fluid saturation pressure.

The work reported here reflects our experience that the EOS is generally not predictive and extensive splitting of the C_{7+} fraction to match laboratory data is generally unnecessary. We indicate that more of the available laboratory data than were frequently used (or reported) in past studies should be used in evaluating and tuning an EOS. The reservoir fluid studies presented illustrate the capability and efficiency of multivariable, nonlinear regression in seeking agreement between EOS and observed PVT results.

We do not dismiss "proper" C_{7+} characterization as a necessary element in tuning an EOS. Rather, we support a philosophy of minimal splitting followed by adjustment, using regression, of the heaviest (plus) fraction's two EOS parameters, generally denoted by Ω_a° and Ω_b°.

We describe regression-based PVT program features that we feel contribute to time-efficient tuning of an EOS, which is necessary before its use in field-scale simulation. Laboratory data given for six oil and three retrograde gas condensate samples include reservoir temperature expansions, surface separations, N_2 reservoir fluid behavior, and one set of multiple-contact data. Results are presented for three additional fluids with data reported in the literature. Generalizations regarding the regression procedure and results, based on these 12 fluid systems and a larger number of unreported fluid studies, are stated where possible or warranted.

Description of the PVT Program

The PVT program is a general-purpose program that uses a generalized cubic EOS[10] to perform phase-equilibrium and property calculations. The generalized EOS reduces to any of the Redlich-Kwong (RK),[11] Soave-Redlich-Kwong (SRK),[12] ZJRK,[13,14] and PR[15] EOS. The program may be used to calculate fluid behavior solely on the basis of the predictive capabilities of any of these equations. More important, however, is the capability to use a nonlinear regression calculation that performs an automatic adjustment of EOS parameters to match a variety of laboratory PVT measurements. The resulting tuned EOS is then used in a compositional reservoir simulator.

The first step in use of the PVT program is to define the components that comprise the fluid system. The program contains an internal table of properties for CO_2, N_2, H_2S, CO, H_2, SO_2, O_2, and pure hydrocarbon components from C_1 through C_{20}. Internally stored binary interaction coefficients closely resemble values given by Yarborough[3] for the RK EOS and by Katz *et al.*[1] for the PR EOS. Properties for user components not contained in this internal table are either entered by the user or determined by interpolation on the basis of molecular weight.

The program also provides the option to split the plus fraction of a sample into a number of extended fractions. The internally stored properties of extended fractions and the method of splitting are those presented by Whitson.[6] In addition to his preservation of molecular weight and mole fraction of the original plus fraction, we added a regression to preserve specific gravity of the plus frac-

*Now with J.S. Nolen & Assocs. Inc.

TABLE 1—FLUID COMPOSITIONS AND PROPERTIES AT RESERVOIR CONDITIONS

	Gas 2*	Gas 2**	Gas 4	Gas 5	Oil 1	Oil 2	Oil 3	Oil 4	Oil 6	Oil 7
CO_2	0.0069	0.0061	0.0350	0.0217	0.0044	0.0090	0.6031	0.0235	0.0103	0.0008
N_2		0.0042	0.0114	0.0034	0.0045	0.0030	0.0093	0.0011	0.0055	0.0164
H_2S	0.0004	0.0004	0.1819							
C_1	0.5832	0.5749	0.5762	0.7064	0.3505	0.5347	0.0705	0.3521	0.3647	0.2840
C_2	0.1355	0.1345	0.0739	0.1076	0.0464	0.1146	0.0157	0.0672	0.0933	0.0716
C_3	0.0761	0.0752	0.0302	0.0494	0.0246	0.0879	0.0306	0.0624	0.0885	0.1048
C_4	0.0403	0.0415	0.0231	0.0302	0.0166	0.0456	0.0331	0.0507	0.0600	0.0840
C_5	0.0241	0.0233	0.0129	0.0135	0.0160	0.0209	0.0268	0.0523	0.0378	0.0382
C_6	0.0190	0.0179	0.0554†	0.0090	0.0546	0.0151	0.0258	0.0410	0.0356	0.0405
C_7	0.1145†	0.1220†		0.0588†	0.4824†	0.1692†	0.0216	0.3497†	0.3043†	0.3597†
C_8							0.0226			
C_9							0.0210			
C_{10}							0.1199†			
$M+$	193	193	117	153	225	173	229	213	200	252
$\gamma+$	0.8135	0.8115	0.7748	0.8100	0.9000	0.8364	0.8570	0.8405	0.8366	0.8429
p_s	4,450	4,415	3,360	4,842	2,520	4,460	2,597	2,547	2,746	1,694
ρ_s	28.85	29.54		19.15	47.96	33.01	44.17	40.34	38.01	44.48
T	190	190	240	267	180	176	179	250	234	131

*Dewpoint sample.
**Bubblepoint sample.
†Plus fraction.

tion. The molar distribution of the single-carbon-number groups in the plus fraction through C_{40} is first determined. A grouping of these single-carbon-number groups into fewer multiple-carbon-number groups then completes the splitting procedure.

In the predictive mode, the program can perform a number of calculations on the basis of the current fluid-system definition as determined by the EOS parameters. For example, these calculations may be performed before and after a regression to compare the EOS-predicted performance with the tuned EOS performance. In addition, following a regression to match data for one or more samples, a prediction of results for one or more different samples may be performed. The calculations available in the PVT program include: (1) saturation pressure and equilibrium-phase properties for a given composition and temperature; (2) density and viscosity calculation for specified pressure, temperature, and composition; (3) constant-composition, constant-volume, and differential expansions for specified sets of pressure levels; (4) single- or multistage flash separation tests; (5) phase-envelope calculations for swelling tests; and (6) pseudoization (lumping) to fewer components. The program uses the Lohrenz *et al.* viscosity correlation[16] with automatic tuning to match experimental viscosity data.

The data to be matched in the nonlinear regression consist of laboratory measurements for one or more fluid samples that may be at the same or different temperatures. Fluid samples from a swelling test that correspond to different mixtures of reservoir fluid and injected gas may also be included. For each sample, the following data may be entered: (1) saturation pressure; (2) densities of oil (gas) and associated gas (liquid) at saturation pressure; (3) K-values at saturation pressure; (4) constant-composition expansion data including relative volume, volume fraction liquid, and gas and liquid gravities; (5) constant-volume expansion data including volume fraction liquid, cumulative gas removed, gas z factor, and oil and gas gravities; (6) differential expansion data including oil FVF, solution gas R_s, z factor, and oil and gas gravities; (7) K-values for any or all of the pressures in any of the expansions; (8) multistage separation data including GOR, oil and gas densities, and K-values for each stage; and (9) swelling-test saturation pressure and volumetric data.

In some cases, as shown by Hoffman *et al.*,[17] the available laboratory data for an oil sample include expansion data for the associated gas phase. The program allows these gas-expansion data to be entered in the oil-sample regression data. In addition, the capability to calculate an exact match of the density of a pure component at a specified pressure and temperature is provided. For example, if injection of pure CO_2 or N_2 or methane were anticipated in the reservoir, the density of that injected gas could be preserved within the context of a simultaneous match of all laboratory data for the fluid system. The set of all observed data for the regression calculation is denoted by $\{d_j\}$, $j=1,2\ldots n_J$.

The regression variables are user-specified and may be any subset of the EOS parameters. These parameters are Ω_{ai}° and Ω_{bi}° for each of the n components and the $n(n-1)/2$ binary interaction coefficients. In addition, the program allows the definition of a single regression variable to represent the average of a range of EOS parameters. This feature is useful when matching data for a fluid system that has an extended analysis. Instead of including a regression variable for each Ω_{ai}° of the extended fraction components, a variable can be defined that represents the Ω_{ai}° of a group of the heavy components. This results in fewer regression variables but still allows each heavy component to contribute to the parameter adjustment process.

The regression is a nonlinear programming calculation that places global upper and lower limits on each regression variable v_i. The user may overread the program default limits to ensure that the variables are allowed to take on only those values that he considers to be physically reasonable. Subject to these limits, the regression determines values of $\{v_i\}$ that minimize the objective function F defined as

$$F=\sum_{j=1}^{n_J} W_j \left| (d_j-d_{jC})/d_j \right| , \quad \ldots\ldots\ldots\ldots\ldots\ldots (1)$$

TABLE 2— EXPANSION AND SEPARATION DATA FOR GAS 2

CCE at 190°F for Dewpoint Sample			CCE at 190°F for Bubblepoint Sample		
p (psig)	V/V_s	f_L (%)	p (psig)	V/V_s	f_L (%)
5,580*	0.9549		5,580*	0.9525	
5,400	0.9607		5,400	0.9589	
5,200	0.9673		5,000	0.9737	
5,000	0.9744		4,800	0.9819	
4,800	0.9819		4,600	0.9916	
4,600	0.9906		4,500	0.9972	
4,500	0.9954		4,450**	1.0000	0.00
4,415**	1.0000	100.00	4,440	1.0005	4.35
4,410	1.0002	74.34	4,420	1.0018	47.38
4,400	1.0009	65.72	4,388	1.0037	50.82
4,380	1.0022	63.23	4,339	1.0068	51.64
4,355	1.0040	60.00	4,300	1.0093	51.94
4,320	1.0064	59.13	4,180	1.0181	51.95
4,287	1.0088	58.48	3,993	1.0372	51.32
4,137	1.0214	57.28	3,780	1.0605	50.07
3,997	1.0344	56.40	3,490	1.1032	47.86
3,887	1.0450	55.29	2,998	1.2053	42.96
3,700	1.0681	53.71	2,505	1.3722	36.75
3,495	1.0960	52.14	2,000	1.6683	28.88
3,012	1.1878	47.21	1,485	2.2378	20.20
2,521	1.3412	40.40	1,058	3.1813	13.06
2,060	1.5879	32.52			
907	3.6456	12.04			

Separator Test for Dewpoint Sample

p (psig)	T (°F)	Separator GOR	Stock-Tank GOR	Stock-Tank Gravity (°API at 60°F)	Specific Gravity of Separator Gas
188	70	3245	165	49.9	0.777

Constant-Volume Expansion at 190° F for Dewpoint Sample

	Reservoir Pressure (psig)							
Component	5580*	4450**	3500	2700	1900	1100	500	0
CO_2+H_2S	0.0073	0.0073	0.0073	0.0073	0.0075	0.0081	0.0092	
C_1	0.5832	0.5832	0.6875	0.7201	0.7341	0.7190	0.6599	
C_2	0.1355	0.1355	0.1345	0.1359	0.1389	0.1502	0.1720	
C_3	0.0761	0.0761	0.0695	0.0644	0.0633	0.0704	0.0895	
C_4	0.0404	0.0404	0.0342	0.0292	0.0272	0.0285	0.0388	
C_5	0.0241	0.0241	0.0162	0.0140	0.0117	0.0113	0.0156	
C_6	0.0190	0.0190	0.0131	0.0079	0.0062	0.0049	0.0069	
C_{7+}	0.1145	0.1145	0.0377	0.0212	0.0111	0.0076	0.0081	
$M+$	193	193	142	128	121	118	119	
z	1.1899	0.9969	0.8402	0.7966	0.8140	0.8603	0.9108	1.0000
G_p	0	0	0.09589	0.22551	0.39165	0.58225	0.72743	0.87957
f_L	0	0	0.5231	0.4940	0.4533	0.4051	0.3682	0.3037

*Original reservoir pressure.
**Saturation pressure.

where d_{jC} and d_j are calculated and observed values of observation j, respectively. The terms W_j are weight factors with internally set default or user-overread values. The default factors are 1.0 with the exceptions of values of 40 and 20 for saturation pressure and density, respectively, at reservoir temperature. If several samples are in a data set, each with saturation pressure and density, then 40 and 20 are used for the first sample and weight factors of 12 and 2 are used for subsequent samples.

The theoretical values of $\Omega_a{}^\circ$, $\Omega_b{}^\circ$ for the PR and RK EOS are roughly 0.4572, 0.0778 and 0.4275, 0.0866, respectively. The default lower and upper regression limits are (0.1, 1.3) for Ω_{ai}° and (0.02, 0.25) for Ω_{bi}°. The default limits on binary interaction coefficients are (−1.0, 0.9). These extremely wide limits are rarely approached in applications and the interpretation of any such approach is discussed in the Appendix. The Appendix also discusses the particular EOS parameters we normally select as regression variables and the justification of their selection.

The nonlinear programming technique is basically an extension of the least-squares, linear programming (LSLP) method.[18] At each iteration of the regression, a local subregion of the global parameter space is defined by $\{(1\pm0.03)v_i\}$ where v_i are last-iterate EOS parameter values. Linearity between $\{d_{jC}\}$ and $\{v_i\}$ values is assumed in this small cubic subregion and the LSLP calculation is performed to calculate new iterate v_i values in this region. If any of the new iterate values lie on a boundary of the subregion, then a new subregion $(1\pm0.03)v_i$ is defined using the new iterate v_i values and

TABLE 3—EXPANSION AND SEPARATION DATA FOR GAS 4

CCE of Reservoir Gas at 240°F			CCE of 4.89% N_2 Mix at 240°F			CCE of 10.47% N_2 Mix at 240°F		
p (psig)	V/V_s	f_L (%)	p (psig)	V/V_s	f_L (%)	p (psig)	V/V_s	f_L (%)
5,500	0.7600		5,500	0.7910		5,500	0.8230	
5,000	0.7901		5,000	0.8271		5,000	0.8611	
4,500	0.8328		4,500	0.8737		4,500	0.9128	
4,000	0.8897		4,000	0.9355		4,200	0.9518	
3,900	0.9031		3,900	0.9503		4,100	0.9669	
3,800	0.9180		3,800	0.9667		4,000	0.9822	
3,700	0.9339		3,700	0.9840		3,895*	1.0000	
3,600	0.9508		3,608*	1.0000		3,700	1.0366	0.58
3,500	0.9670		3,400	1.0445	0.39	3,500	1.0807	1.10
3,360*	1.0000		3,000	1.1577	1.23	3,000	1.2314	2.30
3,200		0.20	2,500	1.3772	3.92	2,500	1.4725	3.43
3,000	1.0936	0.63						
2,500	1.2948	4.61						

CCE of 20.49% N_2 Mix at 240°F			CCE of 30.8% N_2 Mix at 240°F			Partial Phase Diagram of Reservoir Gas	
p (psig)	V/V_s	f_L (%)	p (psig)	V/V_s	f_L (%)	T (°F)	p (psig)
5,500	0.8930		5,500	0.9727		73	2,505
5,000	0.9414		5,400	0.9833		108	2,773
4,800	0.9641		5,250*	1.0000		179	3,175
4,700	0.9768		4,828	1.0525	0.40	193	3,220
4,600	0.9898		4,500	1.1025	0.71	207	3,283
4,528*	1.0000		4,000	1.1996	1.18	220	3,343
4,200	1.0501	0.50	3,500	1.3338	1.68	237	3,360
4,000	1.0865	0.78	2,795	1.6193	2.32	262	3,323
3,500	1.2021	1.48					
3,000	1.3700	2.22					
2,500	1.6237	2.93					

Reservoir Gas Separator Test

p (psig)	T (°F)	Separator GOR**	Separator Liquid Gravity†	Specific Gravity of Separator Gas
188	148	7,465	0.6442	0.812

*Dewpoint pressure.
**Scf separator gas/bbl separator liquid at 1200 psig, 148°F.
†Liquid gravity at 1,200 psig, 148°F.

the LSLP method is applied again. This sequence of iterations converges when all of the new iterate values lie within the latest subregion. Several final iterations are then performed using 1 ± 0.015, 1 ± 0.0075, etc., to reduce the final subregion. This reduction enhances validity of the above-mentioned linearity assumption. The LSLP method obtained d_{jC} as linear functions of $\{v_i\}$ using a least-squares fit of calculated observations from a number of history-match runs. Here we obtain $\{d_{jC}\}$ as linear functions of $\{v_i\}$ by numerical partial differentiation using the EOS.

We do not consider the effects of component pseudoization on EOS calculations in this work. The optimal number and definition of components should be dictated by what process will be carried out in the reservoir.[10] In addition to single-contact (e.g., expansion) laboratory tests, multiple-contact tests and/or reservoir condition flow tests may be necessary to confirm validity of the PVT description.

Definition of Terms

For convenience and brevity in presenting results, several terms are defined here. An average deviation, ϵ, is defined as F^*/n_J, where F^* is the final or converged value of F. This deviation is not equal to the true average deviation because not all weight factors are unity.

The term "predicted" is applied to EOS results calculated with no alteration of any EOS parameters. The term "adjusted" is applied to EOS results calculated after one binary (e.g., $C_1-C_{7+}\times b_{ij}$) is adjusted to match exactly the sample bubblepoint or dewpoint pressure. The term "regressed" is applied to EOS results calculated after a number of EOS parameters have been determined by regression upon a set of laboratory PVT data.

Except where stated otherwise, the regressions described use the five variables of methane $\Omega_a{}^\circ$, $\Omega_b{}^\circ$, plus fraction $\Omega_a{}^\circ$, $\Omega_b{}^\circ$, and the methane-plus fraction binary interaction coefficient. Rationalization of this selection apart from experience is discussed in the Appendix. We refer to the methane-plus-fraction binary simply as the binary, denoted by b or b_{1+}. Its value, determined by EOS adjustment, is referred to as the adjustment binary, denoted by $\hat{b}$. The term "plus fraction" denotes the heaviest component used in the EOS calculations. For example, if the original plus fraction, C_{7+}, of a fluid is split into three fractions, F_7, F_8, and F_9, then F_9 becomes the new plus fraction.

TABLE 4—EXPANSION AND SEPARATION DATA FOR GAS 5

CVE at 267°F — Reservoir Pressure (psig)

Component	4842*	3900	3000	2100	1200	700	700**
CO_2	0.0217	0.0217	0.0220	0.0223	0.0228	0.0233	0.0062
N_2	0.0034	0.0036	0.0038	0.0038	0.0036	0.0034	0.0002
C_1	0.7064	0.7205	0.7365	0.7457	0.7442	0.7338	0.1264
C_2	0.1076	0.1078	0.1087	0.1099	0.1113	0.1134	0.0505
C_3	0.0494	0.0490	0.0485	0.0485	0.0497	0.0518	0.0441
C_4	0.0302	0.0293	0.0283	0.0279	0.0292	0.0313	0.0467
C_5	0.0135	0.0125	0.0118	0.0115	0.0121	0.0135	0.0351
C_6	0.0090	0.0080	0.0072	0.0068	0.0071	0.0081	0.0385
C_{7+}	0.0588	0.0476	0.0332	0.0236	0.0200	0.0214	0.6523
$M+$	153	140	131	125	123	124	171
z	0.985	0.911	0.881	0.882	0.916	0.943	
G_p	0	0.12812	0.29341	0.49110	0.69907	0.81220	
f_L	0	0.0610	0.0910	0.1040	0.0990	0.0910	

CCE at 267°F

p (psig)	V/V_s	Deviation Factor z
7,000	0.8506	1.210
6,500	0.8744	1.155
6,000	0.9035	1.102
5,500	0.9381	1.049
5,300	0.9553	1.030
5,100	0.9732	1.010
5,000	0.9833	1.000
4,900	0.9936	0.990
4,842	1.0000	0.985
4,800	1.0046	
4,700	1.0161	
4,500	1.0429	
4,200	1.0906	
3,900	1.1468	
3,500	1.2444	
3,000	1.4147	
2,600	1.6129	
2,100	1.9851	
1,870	2.2376	
1,675	2.5062	
1,453	2.9132	
1,282	3.3338	
1,143	3.7547	
1,040	4.1757	

Separator Test

p (psig)	T (°F)	Separator GOR	Stock Tank Gravity (°API at 60°F)	Specific Gravity of Separator Gas
425	96	8,933	49.7	0.725

*Dewpoint pressure.
**Residual liquid composition.

TABLE 5—VAPORIZATION AND EXPANSION TEST DATA FOR OIL 1

Vaporization Test at 2520 psig and 180°F

Composition of injected gas: Component	Mol Fraction	Injection Number	Incremental Mols of Gas Injected	Incremental Mols of Gas Produced	Mols of Liquid Phase Remaining	Relative Liquid Volume	CCE of Reservoir Oil at 180°F: p, psig	V/V_s
		0	0.0000	0.0000	1.0000	1.0000		
		1	0.8318	0.8454	0.9864	0.9811		
CO_2	0.0086	2	0.8628	0.8877	0.9615	0.9616	5,000	0.9782
N_2	0.0118	3	0.8067	0.8466	0.9216	0.9434	4,000	0.9862
C_1	0.8898	4	0.8471	0.8728	0.8959	0.9246	3,000	0.9951
C_2	0.0704	5	0.7813	0.7912	0.8860	0.9075	2,900	0.9961
C_3	0.0163	6	0.9017	0.9242	0.8635	0.8889	2,800	0.9971
C_4	0.0024	7	1.0147	0.0407	0.8375	0.8688	2,700	0.9982
C_5	0.0004	8	1.0353	1.0600	0.8128	0.8502	2,600	0.9992
C_6	0.0002	9	0.4800	0.4963	0.7965	0.8409	2,520*	1.0000
C_{7+}	0.0001	10	0.9413	0.9715	0.7663	0.8261		
		11	0.9705	0.9989	0.7379	0.8110		

Hydrocarbon Analyses (mol fraction) of Gases Produced During Vaporization Test at 2520 psig and 180°F

Injection Number / Component	1	2	3	4	5	6	7	8	9	10	11	11**
CO_2	0.0082	0.0082	0.0083	0.0083	0.0083	0.0084	0.0084	0.0084	0.0085	0.0085	0.0085	0.0060
N_2	0.0124	0.0122	0.0120	0.0119	0.0118	0.0117	0.0116	0.0116	0.0115	0.0115	0.0114	0.0020
C_1	0.8748	0.8731	0.8739	0.8738	0.8745	0.8754	0.8760	0.8767	0.8769	0.8771	0.8776	0.3481
C_2	0.0584	0.0650	0.0670	0.0688	0.0693	0.0695	0.0698	0.0701	0.0702	0.0702	0.0703	0.0681
C_3	0.0158	0.0160	0.0161	0.0162	0.0163	0.0163	0.0164	0.0164	0.0164	0.0165	0.0165	0.0279
C_4	0.0057	0.0048	0.0042	0.0039	0.0036	0.0033	0.0031	0.0028	0.0028	0.0027	0.0025	0.0064
C_5	0.0037	0.0027	0.0022	0.0018	0.0016	0.0014	0.0012	0.0010	0.0009	0.0009	0.0009	0.0060
C_6	0.0091	0.0068	0.0055	0.0047	0.0041	0.0036	0.0032	0.0028	0.0027	0.0025	0.0023	0.0204
C_{7+}	0.0119	0.0112	0.0108	0.0106	0.0105	0.0104	0.0103	0.0102	0.0101	0.0101	0.0100	0.5159
$M+$	105	106	107	108	108	109	109	109	109	109	110	258

*Bubblepoint pressure.
**Equilibrium liquid sample at last injection.

TABLE 6—EXPANSION AND SEPARATION DATA FOR OIL 2

	CVE at 176°F							CCE at 176°F	
	Reservoir Pressure, psig								
Component	4460*	3600	2800	2000	1200	600	600**	p (psig)	V/V_s
CO_2	0.0090	0.0126	0.0116	0.0104	0.0104	0.0121	0.0033	6,000	0.9589
N_2	0.0030	0.0049	0.0047	0.0045	0.0041	0.0036		5,500	0.9700
C_1	0.5347	0.6130	0.6766	0.7274	0.7309	0.6992	0.1149	5,000	0.9827
C_2	0.1146	0.1544	0.1439	0.1232	0.1245	0.1404	0.0648	4,900	0.9856
C_3	0.0879	0.1042	0.0878	0.0767	0.0773	0.0867	0.0976	4,800	0.9883
C_4	0.0456	0.0321	0.0341	0.0301	0.0293	0.0340	0.0781	4,700	0.9919
C_5	0.0209	0.0151	0.0109	0.0088	0.0080	0.0090	0.0494	4,600	0.9951
C_6	0.0151	0.0074	0.0044	0.0030	0.0028	0.0033	0.0438	4,500	0.9984
C_{7+}	0.1692	0.0471	0.0260	0.0159	0.0127	0.0117	0.5481	4,460*	1.0000
								4,443	1.0009
$M+$	173	117	108	103	100	102	295	4,305	1.0097
								3,900	1.0412
z		0.798	0.783	0.788	0.843	0.913		3,531	1.0812
G_p	0	0.07535	0.17932	0.32371	0.49908	0.63967		3,132	1.1425
								2,769	1.2232
								2,422	1.3356
								2,128	1.4738
								1,880	1.6384
								1,660	1.8415
								1,351	2.2768
								1,061	2.9892

DE at 176°F

p (psig)	Relative Oil Volume	Solution GOR	Deviation Factor z	Oil Viscosity (cp)	Gas Viscosity (cp)	Oil Density (g/cm³)	Gas Gravity
4,460*	2.921	3377		0.228		0.5300	
4,000	2.343	2351	0.825	0.290	0.0383	0.5632	1.025
3,492	2.059	1814	0.788	0.338	0.0327	0.5883	0.932
3,003	1.886	1471	0.772	0.380	0.0280	0.6082	0.858
2,514	1.756	1205	0.773	0.440	0.0239	0.6262	0.821
2,004	1.645	970	0.790	0.515	0.0202	0.6437	0.799
1,534	1.555	775	0.816	0.602	0.0171	0.6590	0.806
1,001	1.464	573	0.856	0.748	0.0140	0.6752	0.826
505	1.372	383	0.912		0.0120	0.6940	0.888
209	1.298	245	0.958		0.0114	0.7085	1.067
0	1.057	0	0.995	1.547	0.0109	0.7813	1.767

Separator Tests

p (psig)	T (°F)	Separator GOR	Stock-Tank GOR	Stock-Tank Gravity (°API at 60°F)	FVF	Specific Gravity of Separator Gas
300	60	1,597	275	42.6	2.115	0.714
50	60	1,993	68	41.2	2.172	0.805

*Bubblepoint pressure.
**Equilibrium liquid phase.

We refer to constant-composition, constant-volume, and differential expansion data as CCE, CVE, and DE data, respectively. We use the symbol G_p for cumulative gas removed (mol fraction of original) from a cell during a CVE. The symbol f_L denotes volume fraction liquid in a cell during expansion. At each expansion pressure, f_L is liquid volume divided by cell volume at that pressure. For a CCE, the cell volume increases as pressure drops. For a CVE, the cell volume is constant and for a DE, cell volume decreases as pressure decreases.

Gas gravity, γ_g, is simply gas-phase molecular weight divided by the molecular weight of air (28.97). Liquid gravity, γ_L or γ_o, is defined relative to water=1.0 (i.e., γ_L is roughly liquid density in pounds per cubic foot divided by 62.4). Standard cubic feet of gas are defined relative to standard conditions of 14.7 psia [101 kPa] and 60°F [16°C]. All pressures are in units of psia unless stated otherwise.

Sample Data

Tables 1 through 10 list composition, expansion, and separation data for Gases 2, 4, and 5, and Oils 1 through 4, 6, and 7. In these tables, all temperatures are in degrees F, all pressures are in psig, ρ_s is in pounds per cubic foot and viscosities are in centipoises. Unless otherwise noted, separator GOR is standard cubic feet of primary separator gas per stock-tank barrel. For separation test data, single spacing is used to indicate multistage separation. Entries that are double spaced correspond to different separation tests on the same sample. For example, for Oil 4 in Table 8, three different separation tests are given, each consisting of three stages. Following the last entry

TABLE 7—CONSTANT-COMPOSITION EXPANSIONS FOR OIL 3

CCE at 140°F			CCE at 160°F			CCE at 180°F			CCE at 200°F		
p (psig)	V/V_s	f_L (%)	p (psig)	V/V_s	f_L (%)	p (psig)	V/V_s	f_L (%)	p (psig)	V/V_s	f_L (%)
5,000	0.9390		5,000	0.9380		5,000	0.9367		5,000	0.9358	
4,500	0.9466		4,500	0.9464		4,500	0.9461		4,500	0.9463	
4,000	0.9551		4,000	0.9558		4,000	0.9567		4,000	0.9584	
3,500	0.9644		3,500	0.9668		3,500	0.9691		3,500	0.9727	
3,000	0.9752		3,000	0.9791		3,000	0.9844		3,200	0.9829	
2,500	0.9877		2,800	0.9848		2,900	0.9878		3,100	0.9866	
2,400	0.9907		2,700	0.9879		2,800	0.9914		3,000	0.9907	
2,300	0.9937		2,600	0.9911		2,700	0.9956		2,900	0.9948	
2,200	0.9970		2,500	0.9945		2,597*	1.0000	100.0	2,822	0.9986	
2,115*	1.0000	100.0	2,400	0.9984		2,574	1.0032		2,792*	1.0000	100.0
2,092	1.0042		2,362*	1.0000	100.0	2,551	1.0070		2,772	1.0027	
2,068	1.0089		2,350	1.0020		2,536	1.0093	92.7	2,747	1.0070	94.7
2,043	1.0148	94.8	2,328	1.0062		2,521	1.0119	91.7	2,719	1.0117	92.2
1,990	1.0279	89.1	2,307	1.0099		2,492	1.0177	89.9	2,659	1.0229	87.2
1,927	1.0487	85.4	2,270	1.0174	91.1	2,429	1.0319	85.4	2,553	1.0468	80.5
1,834	1.0871	78.8	2,203	1.0319	86.4	2,311	1.0624	78.9	2,355	1.1052	71.2
1,669	1.1862	68.5	2,101	1.0642	80.5	2,126	1.1302	69.8	2,088	1.2194	60.3
1,467	1.3820	54.6	1,968	1.1102	73.9	1,857	1.2795	57.3	1,836	1.3849	50.0
1,308	1.5980	45.0	1,857	1.1765	67.1	1,606	1.4946	46.1	1,682	1.5216	43.8
1,163	1.8705	36.5	1,733	1.2615	60.3	1,391	1.7715	36.8	1,550	1.6684	38.7
1,043	2.1616		1,550	1.4363	50.1	1,223	2.0672		1,390	1.8926	
949	2.4444		1,399	1.6193	42.6	1,091	2.3746		1,239	2.1598	
869	2.7342		1,281	1.8097	36.9	972	2.7187		1,121	2.4242	
817	2.9438	20.6	1,169	2.0406		938	2.8338	20.8	1,013	2.6951	21.7
764	3.1911	18.0	1,030	2.3771		868	3.0877	18.7	943	2.9622	19.3
712	3.4819	15.8	914	2.7532		831	3.2510	17.8	893	3.1517	18.1
653	3.8555		887	2.8669	21.2	788	3.4507	16.5	824	3.4294	
602	4.2312		823	3.1146	19.5	754	3.6307	15.5	757	3.7696	
559	4.6202		784	3.2948	18.4	717	3.8322	14.5	698	4.1252	
			748	3.4885	17.2	663	4.1721		643	4.4922	
$\rho_s = 45.914$			688	3.8349		617	4.5347				
			630	4.2369							
			584	4.6153		$\rho_s = 44.170$			$\rho_s = 43.346$		
			$\rho_s = 45.065$								

*Bubblepoint pressure.

in any separation test, there is an implied final flash to stock-tank conditions of 0 psig [0 kPa], 60°F [16°C]. The reported gravities are separator gas gravities and stock-tank oil gravities unless otherwise noted. Data are given for Gas 1 by Firoozabadi *et al.*,[2] Gas 3 by Vogel and Yarborough,[3] and Oil 5 by Hoffman *et al.*[17]

Because reservoir fluid samples occasionally vary with location and time, these 12 samples may or may not be representative of their respective source fields.

Discussion of Results

The average deviation gives the most concise but least informative comparison of observed and calculated results. Table 11 lists these deviations for the 12 samples after EOS adjustment and regression for both EOS. Regression reduces the adjusted deviation by factors ranging from 17 to only 1.28. In general, the adjusted ZJRK EOS compares better with data than does the adjusted PR EOS. However, the agreement with data after regression is, on the average, slightly better with the PR EOS. For the oil samples, except for Oils 1 and 5, the adjusted ZJRK EOS results compare reasonably well with the data and are improved only moderately by regression.

Table 12 compares experimental and calculated values of a number of PVT quantities pertaining to reservoir temperature expansions and surface separations for the 12 samples. The PR EOS results are listed and the ZJRK EOS results are given in parentheses. For examples with more than one surface separation, the results given are for the lowest-pressure separation. The B_o and R_s values are at bubblepoint. The first and second Gas 2 entries are dewpoint and bubblepoint samples, respectively. The first and second Oil 5 entries correspond to use of 7 and 22 components, respectively, in the calculations. The Oil 3 calculated results used 12 components, through C_{10+}.

The results listed show the rather poor predictive ability of either EOS. In general, the predicted bubblepoint or dewpoint pressures are consistently and significantly low. With only adjustment, the ZJRK EOS yields saturated-oil densities (at bubblepoint pressure and reservoir temperature) and stock-tank oil specific gravities (at 60°F [16°C]) that are consistently higher and significantly more accurate than those from the PR EOS. The table shows that adjustment (changing only the binary) has virtually no effect on stock-tank oil gravity and calculated surface separation results for either EOS.

Surface separation calculations show that both EOS generally predict erroneously low GOR and oil FVF. As stated previously, adjustment does not alter calculated separation results. An obvious question is whether regression only on reservoir temperature data (e.g., expansions) gives EOS reliability under surface separation conditions. Table 13 compares experimental separation results for Oils 5 through 7 with two sets of regressed PR EOS re-

TABLE 8—EXPANSION AND SEPARATION DATA FOR OIL 4

DE at 250°F						DE at 110°F					
p (psig)	Relative Oil Volume	Solution GOR	Deviation Factor z	Oil Density (g/cm³)	Gas Gravity	p (psig)	Relative Oil Volume	Solution GOR	Deviation Factor z	Oil Density (g/cm³)	Gas Gravity
2,547	1.671	932		0.6463		1,958	1.341	701		0.7108	
2,360	1.636	865	0.860	0.6531	0.826	1,753	1.313	633	0.786	0.7174	0.721
2,143	1.595	788	0.859	0.6609	0.824	1,557	1.291	577	0.802	0.7231	0.714
1,893	1.553	704	0.864	0.6695	0.819	1,354	1.264	510	0.820	0.7303	0.709
1,645	1.512	625	0.873	0.6779	0.823	1,153	1.240	450	0.836	0.7370	0.707
1,393	1.473	548	0.883	0.6864	0.828	949	1.217	389	0.854	0.7434	0.710
1,150	1.436	477	0.898	0.6952	0.845	748	1.193	330	0.875	0.7504	0.719
895	1.401	407	0.916	0.7032	0.883	548	1.168	270	0.897	0.7580	0.744
647	1.365	338	0.937	0.7114	0.924	347	1.144	209	0.927	0.7647	0.784
400	1.326	265	0.960	0.7202	1.007	157	1.116	143	0.963	0.7725	0.897
182	1.275	190	0.980	0.7340	1.175	75	1.097	106	0.981	0.7783	1.045
87	1.243	146	0.990	0.7412	1.514	0	1.024	0		0.7994	1.506
0	1.094	0		0.7678	2.551						

CCE at 250°F			CCE at 180°F			CCE at 110°F		
p (psig)	V/V_s	μ_o	p (psig)	V/V_s	μ_o	p (psig)	V/V_s	μ_o
3,500	0.9823		3,000	0.9897		3,000	0.9890	
2,547	1.0000	0.222	2,283	1.0000	0.387	1,958	1.0000	0.635
2,340	1.0363	0.258	2,053	1.0445	0.413	1,785	1.0367	
2,056	1.1033	0.283	1,797	1.1131	0.462	1,535	1.1111	
1,681	1.2381		1,450	1.2585	0.530	1,236	1.2570	0.805
1,294	1.4798		1,147	1.4766	0.585	1,082	1.3737	0.840
650	2.6025	0.473	712	2.1736	0.700	464	2.7743	1.130
473	3.5532		548	2.7825		329	3.8133	
			392	3.7876	0.820			

Separator Tests

p (psig)	T (°F)	Separator GOR	Stock-Tank GOR	Stock-Tank Gravity (°API at 60°F)	Separator Volume Factor	Oil Density (g/cm³)
250	110	551			1.086	0.786
45	110	85			1.056	0.789
0	110		49	41.3	1.025	0.798
250	150	620			1.120	0.768
45	150	80			1.089	0.776
0	150		53	39.7	1.044	0.791
250	180	677			1.145	0.765
45	180	81			1.111	0.767
0	180		52	38.7	1.059	0.784

sults. Regressed Values 1 result from a regression including both reservoir temperature and surface separation data. Regressed Values 2 result from regression only on reservoir temperature data. Table 13 illustrates our general finding that regressed EOS surface separation results are about the same regardless of whether separation data are included in the regression data set.

The degrees of C_{7+} splitting used for these 12 samples ranged from none to four fractions. A general, *a priori* guide to this need is given by the experimentally observed range of C_{7+} molecular weights during an expansion or multiple-contact test. For example, we found C_{7+} splitting into one (no splitting), three, and two fractions advantageous in matching Gases 1, 2, and 3 data, respectively. The experimental ranges of C_{7+} molecular weight were 145 to 110, 199 to 118, and 171 to 123 for Gases 1, 2, and 3, respectively.

Also for any given sample, the anticipated recovery process affects the required degree of splitting. Gas injection processes with vaporization phenomena require somewhat more splitting than depletion/waterflooding processes.

Table 14 shows the final values of the five regression variables for the 12 fluid samples for both the PR and ZJRK EOS. In all cases, the regressions converged to the variable values shown. The adjustment binaries show no correlation with plus-fraction properties. This was also noted by Katz *et al.*[1] in their applications of the PR EOS.

The man-hours spent in studying the 12 samples, including data preparation, ranged from about 6 for Gas 3 to about 20 for Oil 1 and Gas 4. Obviously, required man-hours depend on the engineer's experience and familiarity with the PVT program used, the amount of available data, and difficulties that arise in the matching effort. The rather low man-hours quoted, however, reflect primarily that the regression feature allows rapid evaluation of EOS parameter sets and values.

Gas 1. Gas 1 exhibits a dewpoint pressure of 4,075.4 psia [28 100 kPa] at 180.5°F [82.5°C]. CVE data are given by Firoozabadi *et al.*[2] Published comparisons of data with the PR[2] and a modified RK EOS[8] were obtained by varying the C_{7+} characterization.

A mass balance calculation on the CVE data gives liquid gravities at the five expansion pressures of 1.140, 0.761, 0.696, 0.669, and 0.705. We generally interpret liquid gravities near or above 1.0 as indicative of data error. The regression data set consisted of dewpoint pressure, saturated gas density at that pressure, and values of z_g, G_p, and f_L for each of the five expansion pressures, and excluded gravity and residual liquid K-value data.

TABLE 9—EXPANSION AND SEPARATION DATA FOR OIL 6

DE at 234°F

p (psig)	Relative Oil Volume	Solution GOR	Deviation Factor z	Oil Density (g/cm³)	Gas Gravity
2,746*	1.866	1,230		0.6090	
2,598	1.821	1,151	0.852	0.6162	0.848
2,400	1.771	1,059	0.849	0.6240	0.849
2,200	1.725	972	0.851	0.6314	0.841
1,897	1.658	849	0.858	0.6433	0.836
1,600	1.599	737	0.870	0.6543	0.837
1,300	1.543	631	0.885	0.6655	0.846
1,000	1.488	529	0.906	0.6767	0.872
700	1.433	428	0.925	0.6888	0.920
394	1.371	321	0.951	0.7028	1.038
195	1.313	231		0.7145	1.248
112	1.274	178		0.7231	1.458
0	1.086	0		0.7687	2.245

CCE at 234°F

p (psig)	V/V_s
5,000	0.9581
4,500	0.9655
4,000	0.9738
3,500	0.9829
3,200	0.9892
3,100	0.9915
3,000	0.9937
2,900	0.9961
2,800	0.9986
2,746*	1.0000
2,734	1.0023
2,721	1.0042
2,692	1.0090
2,605	1.0218
2,500	1.0410
2,362	1.0697
2,203	1.1082
2,012	1.1661
1,815	1.2432
1,608	1.3497
1,415	1.4853
1,225	1.6697
968	2.0395
742	2.6216
535	3.5732

Separator Tests

p (psig)	T (°F)	Separator GOR	Stock-Tank GOR	Stock-Tank Gravity (°API at 60°F)	FVF	Specific Gravity of Separator Gas
0	74	1,059		40.9	1.722	0.996
50	74	874	53	42.4	1.627	
100	74	810	100	42.7	1.610	
200	74	722	188	42.6	1.611	

*Bubblepoint pressure.

TABLE 10—EXPANSION AND SEPARATION DATA FOR OIL 7

DE at 131°F

p (psig)	Relative Oil Volume	Solution GOR	Deviation Factor z	Oil Density (g/cm³)	Gas Gravity
1,694*	1.324	557		0.7126	
1,550	1.311	526	0.718	0.7157	0.854
1,400	1.298	493	0.717	0.7190	0.860
1,252	1.285	460	0.716	0.7223	0.869
1,100	1.270	423	0.716	0.7265	0.880
950	1.256	389	0.718	0.7300	0.889
798	1.240	349	0.726	0.7345	0.905
643	1.224	310	0.736	0.7392	0.914
500	1.209	273	0.755	0.7434	0.927
350	1.188	229	0.806	0.7498	0.940
200	1.160	179	0.918	0.7594	0.958
102	1.136	137	1.117	0.7663	
0	1.034	0	1.513	0.7981	

CCE at 131°F

p (psig)	V/V_s
5,000	0.9707
4,500	0.9743
4,000	0.9784
3,500	0.9825
3,000	0.9871
2,500	0.9917
2,100	0.9957
2,000	0.9968
1,900	0.9978
1,800	0.9989
1,700	0.9999
1,694*	1.0000
1,682	1.0028
1,670	1.0048
1,642	1.0100
1,572	1.0242
1,475	1.0477
1,377	1.0764
1,263	1.1183
1,128	1.1814
1,000	1.2656
870	1.3816
750	1.5296
588	1.8573
462	2.2664
352	2.9035
258	3.9479

Separator Tests

p (psig)	T (°F)	Separator GOR	Stock-Tank GOR	Stock-Tank Gravity (°API at 60°F)	FVF	Specific Gravity of Separator Gas
0	72	580		39.7	1.340	1.075
40	72	472	43	41.5	1.306	
80	72	424	80	41.6	1.299	
160	72	366	142	41.5	1.302	

*Bubblepoint pressure.

TABLE 11—AVERAGE DEVIATIONS, SAMPLES 1 THROUGH 12 (%)

			PR EOS		ZJRK EOS	
Sample	n_C	n_J	Adjusted	Regressed	Adjusted	Regressed
Gas 1	9	17	32.50	1.50	31.10	1.47
Gas 2	9	57	29.49	6.20	28.42	6.08
Gas 2	11	57	12.48	5.01	9.20	4.05
Gas 3	10	13	50.83	1.79	44.35	1.83
Gas 4	12	11	48.00	0.67	59.40	1.02
Gas 5	9	42	17.07	6.73	15.61	7.16
Gas 5	10	42	13.09	6.01	9.75	5.52
Oil 1	9	57	12.12	2.88	7.28	2.77
Oil 1	10	57	6.42	0.31	3.33	0.27
Oil 2	9	79	10.25	4.68	7.25	5.66
Oil 2	11	79	—	2.71	—	—
Oil 3	9	46	9.20	2.58	8.47	4.87
Oil 3	12	46	9.07	2.03	6.37	3.97
Oil 4	9	169	9.70	2.69	4.57	2.28
Oil 5	7	19	28.30	2.19	25.37	1.78
Oil 5	22	19	18.89	3.89	5.91	1.80
Oil 6	9	75	12.00	2.10	3.97	2.67
Oil 7	9	76	8.08	4.14	5.58	4.08
Average			19.26	3.26	16.23	3.36

Fig. 1 compares regressed PR EOS results with data and results of the above-mentioned studies. Our results compare rather well with the data with the exception of the z_g values. The regression used the given nine-component analysis with no splitting of the C_{7+} plus fraction. A regression with C_{7+} split into three fractions did not improve the match. Table 15 shows reasonably good agreement between experimental and regressed PR CVE residual liquid compositions. The Firoozabadi *et al.* results[2] used an extended analysis to C_{16+}.

Table 11 shows that both EOS gave an average deviation of about 32% after adjustment and a deviation of about 1.5% after regression. Table 14 gives the reasonable $\Omega_a°$, $\Omega_b°$ values and large methane/C_{7+} binary above 0.4 determined by regression. The two EOS gave very similar results. Predicted dewpoint pressures were 3,334 and 3,461 psia [22 987 and 23 863 kPa] for the PR and ZJRK EOS, respectively, compared with the observed 4,075.4 psia [28 100 kPa].

Gas 2. Gas 2 is a fluid virtually at its critical point at reservoir temperature of 190°F [87.8°C]. Because of the possibility of a small error in gas measurement during well testing, two slightly different separator gas/liquid ratios were used to obtain the two reservoir fluid compositions given in Table 1. One sample exhibited a dewpoint pressure of 4,465 psia [30 785 kPa], the other a bubblepoint of 4,430 psia [30 544 kPa] at 190°F [87.8°C]. Table 2 gives CCE data for the bubblepoint sample and CCE, CVE, and separation data for the dewpoint sample.

Fig. 2 compares experimental CCE results with those calculated from the PR EOS after regression with C_{7+} split into three fractions. Fig. 3 compares CVE observed results with PR and ZJRK calculated results for the dewpoint sample. Where the triangular ZJRK points are not shown, they coincide with the circular PR points. The PR match is good with the exception of z_g and γ_L disparities. The ZJRK results are slightly better overall, as in-

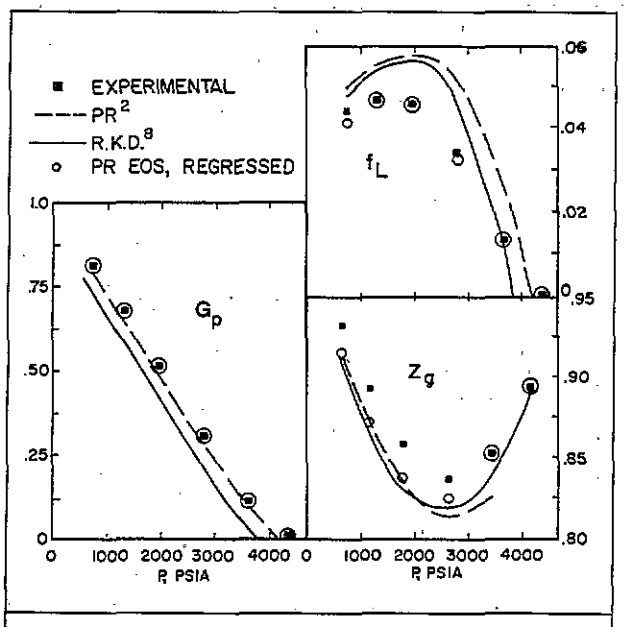

Fig. 1—Gas 1 CVE at 180.5°F.

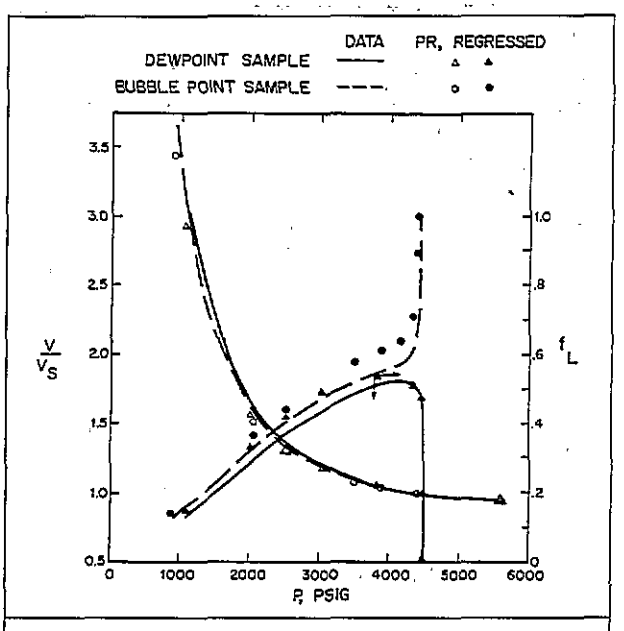

Fig. 2—Gas 2 CCE's.

TABLE 12—EXPERIMENTAL AND CALCULATED FLUID SAMPLE PROPERTIES

Property	Sample	T (°F)	Experimental	Predicted	Adjusted	Regressed
Saturation pressure (psia)	Gas 1	181	4,076	3,334 (3,461)	4,076 (4,076)	4,076 (4,076)
	Gas 2	190	4,465	3,680 (3,593)	4,465 (4,465)	4,465 (4,465)
	Gas 2	190	4,430	3,664 (3,571)	4,386 (4,332)	4,403 (4,427)
	Gas 3	226	4,453	4,547 (4,857)	4,453 (4,453)	4,453 (4,453)
	Gas 4	240	3,375	3,138 (3,246)	3,375 (3,375)	3,375 (3,375)
	Gas 5	267	4,857	4,494 (4,165)	4,857 (4,857)	4,857 (4,857)
	Oil 2	176	4,475	3,344 (3,477)	4,475 (4,475)	4,475 (4,475)
	Oil 3	140	2,130	1,761 (1,818)	2,130 (2,130)	2,130 (2,130)
		160	2,377	1,985 (2,014)	2,355 (2,324)	2,376 (2,373)
		180	2,612	2,195 (2,200)	2,560 (2,506)	2,602 (2,598)
		200	2,807	2,388 (2,375)	2,744 (2,674)	2,807 (2,807)
	Oil 4	110	1,973	1,679 (1,805)	2,073 (2,180)	1,967 (1,950)
		180	2,298	2,018 (2,100)	2,371 (2,421)	2,319 (2,308)
		250	2,562	2,259 (2,300)	2,562 (2,562)	2,562 (2,562)
Density at saturation pressure (lbm/cu ft)	Oil 5	201	3,837	3,284 (3,342)	3,837 (3,837)	3,837 (3,837)
	Oil 5	201	3,837	3,311 (3,366)	3,837 (3,837)	3,837 (3,837)
	Oil 6	234	2,761	2,383 (2,432)	2,761 (2,761)	2,761 (2,761)
	Oil 7	131	1,709	1,531 (1,631)	1,709 (1,709)	1,709 (1,709)
	Gas 1	181	15.8	14.3 (14.4)	16.3 (15.9)	15.8 (15.8)
	Gas 2	190	28.8	27.8 (28.2)	29.0 (29.4)	28.8 (28.8)
	Gas 2	190	29.5	28.3 (28.7)	29.3 (29.8)	29.2 (29.3)
	Gas 4	240		16.6 (16.8)	16.6 (16.7)	18.6 (17.6)
	Gas 5	267	19.2	19.2 (18.1)	20.0 (19.5)	19.2 (19.2)
	Oil 2	176	33.1	31.1 (32.2)	32.3 (33.1)	33.1 (33.1)
	Oil 3	140	45.9	43.1 (46.5)	43.5 (46.7)	45.9 (45.9)
		160	45.1	42.3 (45.6)	42.7 (45.9)	45.1 (45.3)
		180	44.2	41.5 (44.8)	42.0 (45.1)	44.3 (44.6)
		200	43.3	40.6 (44.0)	41.1 (44.3)	43.5 (43.9)
	Oil 4	110	44.4	40.0 (43.8)	40.1 (43.9)	43.7 (44.2)
		180	42.4	38.4 (41.7)	38.6 (41.9)	42.1 (42.4)
		250	40.3	36.8 (39.5)	37.0 (39.6)	40.3 (40.3)
	Oil 5	201	41.6	37.3 (40.2)	37.6 (40.5)	41.6 (41.6)
	Oil 5	201	41.6	37.4 (40.3)	37.7 (40.6)	
	Oil 6	234	38.0	35.6 (37.7)	35.9 (38.0)	38.0 (38.0)
	Oil 7	131	44.5	40.7 (44.9)	40.8 (44.9)	44.5 (44.5)
FVF at bubblepoint pressure (RB/STB)	Oil 2	176	2.921	2.419 (2.641)	2.368 (2.607)	2.948 (2.966)
	Oil 4	110	1.341	1.294 (1.353)	1.289 (1.348)	1.355 (1.354)
		250	1.671	1.517 (1.638)	1.508 (1.631)	1.597 (1.609)
	Oil 6	234	1.866	1.659 (1.802)	1.646 (1.791)	1.883 (1.895)
	Oil 7	131	1.324	1.296 (1.365)	1.294 (1.364)	1.300 (1.325)
Solution gas at bubblepoint pressure (scf/STB)	Oil 2	176	3,377	2,550 (2,880)	2,602 (2,939)	3,378 (3,378)
	Oil 4	110	701	611 (702)	612 (703)	703 (714)
		250	932	756 (878)	757 (878)	876 (883)
	Oil 6	234	1,230	1,002 (1,155)	1,003 (1,156)	1,238 (1,230)
	Oil 7	131	557	542 (633)	543 (633)	598 (612)
FVF, B_{oF}, from surface separation (RB/STB)	Oil 2		2.172	2.052 (2.303)	2.050 (2.300)	2.386 (2.463)
	Oil 4	110	1.467	1.276 (1.461)	1.276 (1.461)	1.461 (1.475)
		150	1.520	1.306 (1.503)	1.306 (1.502)	1.499 (1.516)
		180	1.563	1.329 (1.533)	1.330 (1.533)	1.529 (1.546)
	Oil 5	77	1.475	1.238 (1.427)	1.238 (1.427)	1.404 (1.475)
	Oil 5	77	1.475	1.247 (1.436)	1.247 (1.436)	
	Oil 6	74	1.722	1.487 (1.704)	1.487 (1.705)	1.730 (1.783)
	Oil 7	72	1.340	1.187 (1.380)	1.188 (1.380)	1.302 (1.328)
Solution gas from surface separation, R_{sF} (scf/STB)	Gas 2*	70	3,410			3,092 (3,497)
	Gas 4**	148	7,465	7,796 (7,613)	8,315 (7,940)	7,465 (7,465)
	Gas 5†	96	8,933	8,407 (8,504)	8,408 (8,502)	8,894 (8,933)
	Oil 2		2,061	2,189 (2,460)	2,185 (2,454)	2,543 (2,626)
	Oil 4	110	685	604 (693)	603 (692)	693 (705)
		150	753	649 (750)	649 (749)	748 (762)
		180	810	683 (791)	682 (790)	788 (803)
	Oil 5	77	910	752 (867)	752 (868)	855 (898)
	Oil 5	77	910	760 (876)	761 (877)	
	Oil 6	74	1,059	910 (1,046)	911 (1,046)	1,061 (1,093)
	Oil 7	72	580	545 (635)	546 (635)	601 (615)
Stock-tank oil gravity from DE	Oil 2	60	0.827	0.709 (0.803)	0.709 (0.803)	0.837 (0.868)
	Oil 4	110	0.820	0.711 (0.815)	0.712 (0.815)	0.814 (0.820)
		250	0.841	0.717 (0.830)	0.717 (0.830)	0.827 (0.834)
	Oil 6	60	0.835	0.715 (0.823)	0.715 (0.824)	0.837 (0.864)
	Oil 7	60	0.826	0.722 (0.838)	0.722 (0.838)	0.790 (0.804)

TABLE 12—Continued

Property	Sample	T (°F)	Experimental	Predicted	Adjusted	Regressed
Stock-tank oil gravity from surface separation	Gas 2	70	0.780			0.789 (0.829)
	Gas 4	148		0.619 (0.623)	0.628 (0.628)	0.620 (0.615)
	Gas 5	96	0.781	0.765 (0.744)	0.765 (0.773)	0.805 (0.805)
	Oil 2	60	0.819	0.703 (0.787)	0.703 (0.787)	0.817 (0.843)
	Oil 4	110	0.819	0.711 (0.814)	0.711 (0.814)	0.813 (0.819)
		150	0.827	0.713 (0.819)	0.713 (0.819)	
		180	0.831	0.714 (0.823)	0.714 (0.823)	0.821 (0.827)
	Oil 5	60		0.715 (0.824)	0.715 (0.824)	0.809 (0.850)
	Oil 5	60		0.717 (0.827)	0.717 (0.827)	
	Oil 6	60	0.821	0.712 (0.816)	0.712 (0.816)	0.828 (0.854)
	Oil 7	60	0.827	0.722 (0.838)	0.722 (0.838)	0.790 (0.805)
R_{sF} ‡	Oil 5	201	35,120	82,089 (106,550)	69,283 (85,361)	35,120 (33,591)
	Oil 5	201	35,120	43,257 (47,952)	29,933 (34,227)	

*Separator plus stock-tank gas, scf/STB.
**Scf separator gas/bbl liquid at 1,215 psia, 148°F.
†Scf primary separator gas/STB at 60°F.
‡GOR for flash of associated gas at 800 psia, 83°F.

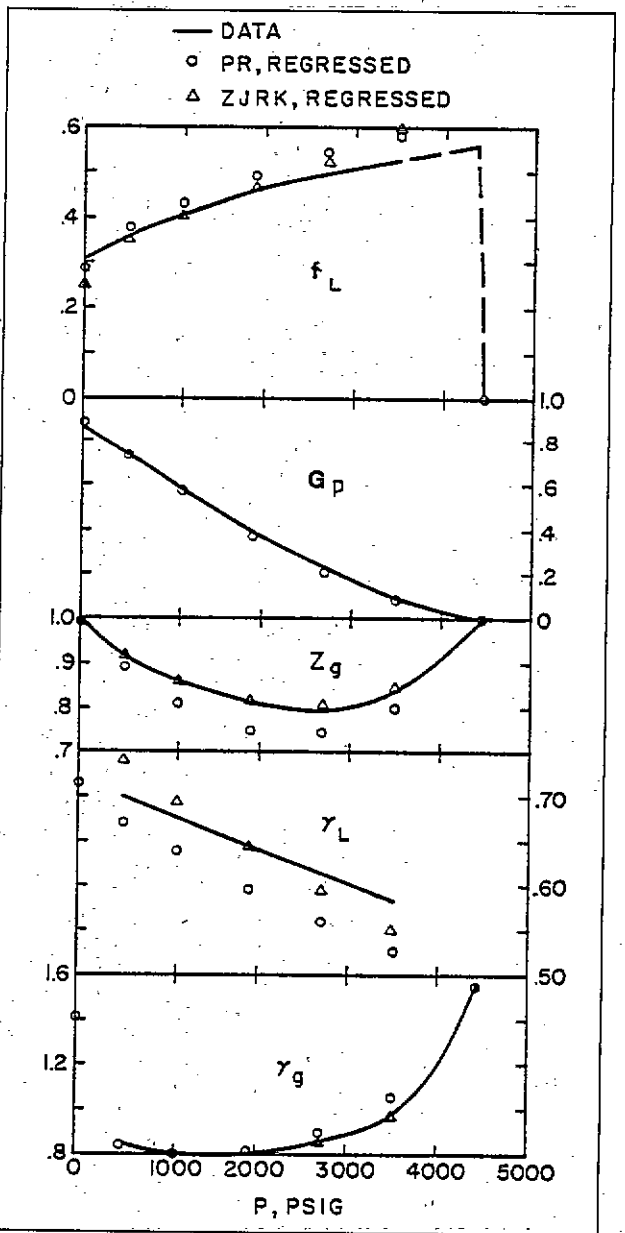

Fig. 3—Gas 3 CVE dewpoint sample at 190°F.

dicated by the 4% average deviation compared to the 5% PR deviation shown in Table 11.

The regression data set excluded K-value data from the reported CVE gas and residual liquid compositions at 514.7 psia [3548.7 kPa]. Table 6 shows that the regressed PR EOS gives good agreement with the experimental liquid compositions. The ZJRK EOS gives equally good agreement. The regression data set also excluded two-stage separation data for the dewpoint sample. Table 16 compares PR and ZJRK EOS results with those data. Table 12 shows the poor predictions of dewpoint pressures obtained from both EOS.

As shown in Table 11, the average deviation with adjustment was reduced more than two-fold by regression; splitting the C_{7+} resulted in better agreement between EOS and experimental results. Table 14 shows that, generally, large methane Ω values and small plus-fraction Ω values were obtained in regression on Gas 2. We feel that slight changes in sample compositions within the realm of experimental error might have a large impact on these regression-variable values.

A mass balance on the dewpoint-sample CVE data gave very reasonable liquid-gravity values. The regression data set included these γ_L values and available γ_g, z_g, f_L, and G_p values for each of the six CVE pressure steps. It also included saturation pressure and density and CCE relative volume and f_L data for both samples.

The proximity to critical of the Gas 2 compositions is indicated by the K-values for the dewpoint and bubblepoint samples at their respective saturation pressures shown in Table 17 that were calculated by the PR EOS after regression.

Gas 3. Gas 3 is Vogel and Yarborough's[5] "Gas 1." Dewpoint pressure is 4,453 psia [30 702 kPa] at 225.8°F [108°C]. They presented plots that compared observed values with their RK EOS-calculated value of liquid dropout for the reservoir fluid and for 10, 30, and 50% N_2 mixes. Their 30 N_2 mix, for example, is a mixture of 0.7 moles of reservoir gas with 0.3 moles of N_2.

Vogel and Yarborough used 42 components in their EOS, splitting the C_{7+} fraction (9.05 mol%) into fractions C_7 through C_{40}. They tuned this extended analy-

TABLE 13—SURFACE SEPARATION DATA AND RESULTS FOR OILS 5 THROUGH 7

Separation Conditions p,T (psig,°F)	Property	Experimental	Regressed*	Regressed**
		Oil 5		
785, 83	GOR†	35,120	35,120	36,256
	γ_g		0.6047	0.6045
	γ_o		0.7424	0.7420
0, 60	GOR	910	855	854
	γ_g		0.6905	0.6889
	γ_o		0.8085	0.8076
	B_o	1.475	1.404	1.402
		Oil 6		
200, 74	GOR	722	727	726
	γ_o	0.8128	0.8128	0.8123
	B_o	1.611	1.606	1.605
100, 74	GOR	810	804	804
	γ_o	0.8123	0.8123	0.8118
	B_o	1.610	1.603	1.602
50, 74	GOR	874	874	873
	γ_o	0.8137	0.8141	0.8136
	B_o	1.627	1.612	1.617
0, 74	GOR	1059	1061	1060
	γ_g	0.9960	0.9788	0.9789
	γ_o	0.8208	0.8275	0.8270
	B_o	1.722	1.730	1.729
		Oil 7		
160, 72	GOR	366	382	379
	γ_o	0.8179	0.7835	0.7786
	B_o	1.302	1.242	1.234
80, 72	GOR	424	439	435
	γ_o	0.8174	0.7831	0.7782
	B_o	1.299	1.238	1.230
40, 72	GOR	472	487	484
	γ_o	0.8179	0.7839	0.7790
	B_o	1.306	1.246	1.237
0, 72	GOR	580	600	596
	γ_g	1.075	1.053	1.052
	γ_o	0.8265	0.7903	0.7853
	B_o	1.340	1.302	1.293

*Regressed results including data at both reservoir and surface conditions.
**Regressed results including only reservoir data. Surface separation results are based upon the match of reservoir data only.
†GOR resulting from flash of gas associated with bubblepoint oil, primary separator scf/STB.

sis with the reservoir gas data and then calculated good agreement with observed liquid dropout data for that gas and the three N_2 mixes.

Fig. 4 compares observed results with our regressed, 10-component PR EOS results for Gas 3 and its three N_2 mixes. The agreement with data is comparable to that obtained by Vogel and Yarborough. The C_{7+} was split into two fractions and the five regression variables were the usual methane and plus-fraction Ω's and the methane/plus-fraction binary. Table 14 shows the reasonable values found by regression. No N_2 EOS parameters were altered or regressed. The regression data set included Gas 3 dewpoint and liquid dropout data and the single additional data point of 8,006 psia [55 200 kPa] dewpoint pressure for the 30% N_2 mix.

For both EOS, the average deviation fell from over 40% after adjustment to about 1.8% after regression, as shown in Table 11. The regressed ZJRK results agree with the data on Fig. 4 equally as well as the PR results. The agreement shown on Fig. 4 is only slightly poorer when the 30% N_2 mix dewpoint is excluded from the regression data set.

No relative volume, dewpoint fluid density, or usable surface separation data were given by Vogel and Yarborough. In cases of missing density data, we closely examine the liquid gravities calculated after regression. If poor data or EOS inadequacy has resulted in unrealistic parameter values, this will frequently appear in the form of obviously erroneous calculated CCE or CVE liquid gravities. In this case, both EOS calculated very reasonable liquid gravities at reservoir temperature, increasing (with decreasing pressure) from about 0.52 to 0.7 for the reservoir gas expansion. At any given intermediate pressure, liquid gravity increased significantly with increasing N_2 content. However, the highest calculated gravity, for 50% N_2 at 1,015 psia [6998 kPa], was 0.770.

When the methane-plus fraction binary was omitted from the variable set for Gas 3, the methane Ω_a° value

TABLE 14—FINAL VALUES OF REGRESSION VARIABLES

Sample	n_C	$\hat{b}$	Ω^o_{a1}	Ω^o_{a2}	Ω^o_{a+}	Ω^o_{b+}	b_{1+}
PR EOS							
Gas 1	9	0.140	0.420	0.069	0.430	0.097	0.408
Gas 2	9	0.094	0.708	0.108	0.264	0.058	0.200
Gas 2	11	0.272	0.600	0.096	0.391	0.054	0.037
Gas 3	10	0.021	0.494	0.069	0.278	0.051	0.156
Gas 4	12	0.089*	0.493	0.073	0.285	0.042	0.054**
Gas 5	9	0.177	0.593	0.091	0.342	0.065	0.295
Gas 5	10	0.116	0.577	0.096	0.342	0.064	0.191
Oil 1	9	0.135	0.501	0.085	0.763	0.069	−0.211
Oil 1	10	0.056	0.449	0.082	0.464†	0.056†	−0.186
Oil 2	11	0.137	0.323	0.064	0.539	0.090	0.178
Oil 3	9	0.142	0.438	0.078	0.529	0.081	0.084
Oil 3	12	0.141	0.436	0.080	0.420	0.069	0.072
Oil 4	9	0.109	0.554	0.105	0.411	0.067	−0.054
Oil 5	7	0.092	0.382	0.050	0.288	0.066	0.284
Oil 5	22	0.253	0.396	0.067	0.347	0.044	0.056**
Oil 6	9	0.117	0.313	0.065	0.478	0.087	0.157
Oil 7	9	0.092	0.482	0.071	0.371	0.075	−0.100
ZJRK EOS							
Gas 1	9	0.101	0.421	0.077	0.382	0.105	0.434
Gas 2	9	0.038	0.629	0.110	0.257	0.069	0.212
Gas 2	11	0.299	0.488	0.103	0.226	0.045	0.058
Gas 3	10	0.079	0.453	0.085	0.310	0.058	−0.030
Gas 4	12	0.094*	0.521	0.095	0.329	0.056	0
Gas 5	9	0.143	0.509	0.090	0.320	0.077	0.350
Gas 5	10	0.148	0.549	0.103	0.434	0.075	−0.017
Oil 1	9	0.073	0.445	0.088	0.798	0.087	−0.233
Oil 1	10	0.043	0.425	0.087	0.518†	0.075†	−0.104
Oil 2	11	0.086	0.344	0.079	0.500	0.095	0.151
Oil 3	9	0.146	0.361	0.063	0.616	0.105	0.150
Oil 3	12	0.147	0.382	0.074	0.610	0.103	0.134
Oil 4	9	0.052	0.475	0.096	0.504	0.087	−0.058
Oil 5	7	0.039	0.428	0.051	0.328	0.085	0.318
Oil 5	22	0.182	0.414	0.083	0.576	0.082	0**
Oil 6	9	0.061	0.363	0.082	0.488	0.098	0.102
Oil 7	9	0.017	0.539	0.092	0.343	0.071	−0.050

*Methane Ω^o_a value.
**This binary was fixed and not regressed upon.
†Values for Ω^o_{a10}, Ω^o_{b10}. Regression also included Ω^o_{a9}, Ω^o_{b9}.

converged to a value near 1.1. Such wide departure of a regression variable from its theoretical value can result from poor data, EOS inadequacy, too many regression variables, or too few regression variables. In this case the cause was too few regression variables. Addition of the methane-plus fraction binary resulted in converged, reasonable values of all regression variables.

Gas 4. Gas 4 exhibits a dewpoint of 3,375 psia [23 270 kPa] at 240°F [116°C] and 134 bbl [21.3 m^3] of separator liquid at 1,215 psia [8377 kPa] at 148°F [64°C] per 1×10^6 scf [28 317 std m^3] of separator gas. The reservoir fluid composition through C_{6+} given in Table 7 shows an H_2S mol fraction of 0.1819. Available data include reservoir fluid dewpoint vs. temperature from 73 to 262°F [24 to 128°C], dewpoint vs. mol% N_2 for four mixes of reservoir fluid and N_2, and CCE data including liquid dropout values for the reservoir fluid and the four N_2 mixes at 240°F [116°C]. These data are given in Table 3. The 4.89% N_2 mix is to be interpreted as a mixture of 4.89 moles of N_2 with 95.11 moles of reservoir gas.

TABLE 15—CVE RESIDUAL LIQUID COMPOSITIONS (MOL%)

	Gas 1 $p=696.2$ psia		Gas 2 $p=514.7$ psia		Gas 5 $p=714.7$ psia	
	Experimental	Calculated	Experimental	Calculated	Experimental	Calculated
CO_2	0.82	1.06	—	0.62	0.57	—
C_1	15.65	12.88	8.49	9.36	12.66	11.51
C_2	3.62	4.04	6.95	6.61	5.05	4.24
C_3	3.88	4.01	9.07	8.15	4.41	3.62
C_4	4.63	5.11	7.97	7.69	4.67	4.46
C_5	5.48	5.92	6.54	6.68	3.51	3.44
C_6	6.44	6.55	6.44	6.58	3.85	3.68
C_{7+}	59.48	60.43	54.54	54.70	65.23	68.47

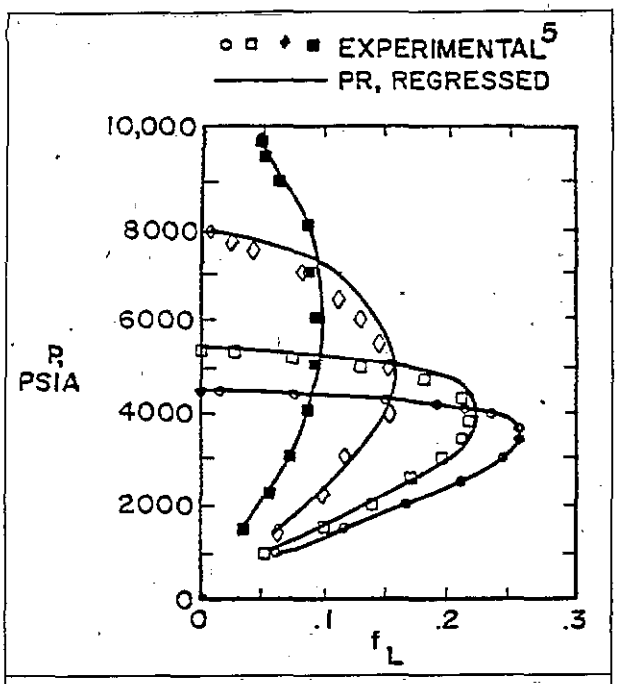

Fig. 4—Gas 3 N_2 mix CCE at 225.8°F.

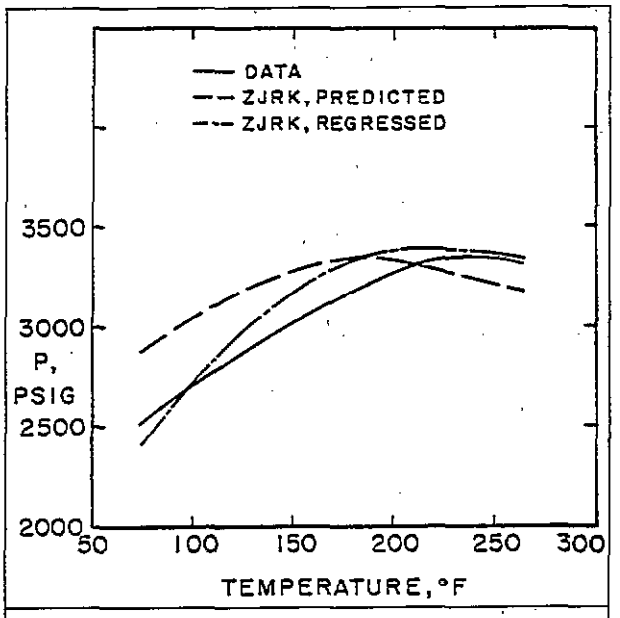

Fig. 5—Gas 4 dewpoint pressure vs. temperature.

All calculated results presented were obtained with a splitting of the C_{6+} into four fractions. Splitting into fewer fractions resulted in a poorer match of data and splitting into more fractions did not improve the match. The methane Ω_b^o value was used as the single regression variable for adjustment in place of the methane-plus fraction binary. This was done because the splitting of C_{6+} gave a plus fraction of only 0.088 mol%. The regression data set included only reservoir-fluid CCE and single-stage surface separation data. No temperature-dependent dewpoint data or N_2 mix CCE or dewpoint data were included in the set.

Table 11 shows that both EOS give average deviations of about 50% after adjustment. Regression lowers those deviations markedly to 1.02 and 0.67% for the ZJRK and PR EOS, respectively. Fig. 5 shows that the ZJRK EOS reproduces the observed dewpoint pressure variation with temperature somewhat better after regression, even though no temperature-dependent dewpoint data were in the regression data set. The PR EOS, after regression, gave a somewhat better match of this temperature dependence than did the ZJRK EOS.

Fig. 6 shows that the ZJRK EOS match of dewpoint pressure vs. mol% N_2 is poor without regression and very good with regression, even though no N_2 dewpoint data or N_2 EOS parameters were used in the regression. The regressed PR results are comparable with these ZJRK results.

Fig. 7 shows good agreement between observed and calculated CCE relative volume results for the original reservoir fluid and the four N_2 mixes. However, Fig. 8 shows rather poor agreement between observed and calculated CCE liquid dropout curves. All calculated results shown are for the regressed ZJRK EOS. The regressed PR EOS results are insignificantly different. The regressed EOS matches the reservoir fluid liquid dropout nearly exactly but seriously underestimates the amount of liquid dropout near dewpoint pressures as N_2 is added to the

TABLE 16—COMPARISON OF CALCULATED AND OBSERVED TWO-STAGE SURFACE SEPARATION RESULTS

	n_C	GOR	Stock-tank γ_L	Primary Separator γ_g
Gas 2 Primary Separator: 202.7 psia, 70°F				
Experimental		3410*	0.780	0.777
PR	9	3689	0.878	0.754
PR	11	3092	0.731	0.754
ZJRK	9	3849	0.916	0.754
ZJRK	11	3497	0.829	0.752
Gas 5 Primary Separator: 439.7 psia, 96°F				
Experimental		8933**	0.781	0.725
PR	9	8819	0.800	0.722
PR	10	8894	0.805	0.722
ZJRK	9	9049	0.821	0.721
ZJRK	10	8933	0.805	0.723

*Separator plus stock-tank gas scf/STB at 60°F.
**Separator gas scf/STB at 60°F.

TABLE 17—K-VALUES FOR GAS 2 DEWPOINT AND BUBBLEPOINT SAMPLES

Component	Dewpoint Sample	Bubblepoint Sample
CO_2	1.00198	1.00908
C_1	1.00602	1.02795
C_2	1.00126	1.00564
C_3	0.99819	0.99118
C_4	0.99533	0.97797
C_5	0.99277	0.96610
C_6	0.98994	0.95317
F_7	0.98214	0.91816
F_8	0.97330	0.87881
F_9	0.93465	0.72346

TABLE 18—FLUID COMPOSITIONS AT LAST INJECTION STEP FOR OIL 1

	Liquid			Gas		
Component	Experimental	PR no split	PR split	Experimental	PR no split	PR split
CO_2	0.0060	0.0037	0.0048	0.0085	0.0086	0.0086
N_2	0.0022	0.0012	0.0019	0.0114	0.0118	0.0116
C_1	0.3480	0.3829	0.3425	0.8776	0.8887	0.8800
C_2	0.0680	0.0372	0.0523	0.0703	0.0703	0.0704
C_3	0.0279	0.0141	0.0217	0.0165	0.0163	0.0165
C_4	0.0064	0.0037	0.0062	0.0025	0.0024	0.0026
C_5	0.0051	0.0013	0.0031	0.0009	0.0006	0.0008
C_6	0.0204	0.0043	0.0147	0.0023	0.0013	0.0024
C_{7+}	0.5159	0.5516	0.5528	0.0100	0.0000	0.0070

reservoir fluid. The liquid dropout data match was not improved by including N_2 Mix 4 CCE data in the regression data set and N_2 Ω_a°, Ω_b° values in the variable set. Because of the small plus-fraction mol fraction after splitting, the regression variable set included only the four variables of methane and plus-fraction Ω_a°, Ω_b°. Table 14 lists the values of these variables converged on by regression.

Both regressed EOS calculated separator GOR and liquid gravity (at separator conditions) as 7465 scf/bbl [1345 std m^3/m^3] separator liquid and 0.615, respectively, compared to observed values of 7465 scf/bbl [1345 std m^3/m^3] and 0.644.

Many variations of regression data and variable sets and degrees of splitting were tried without improvement in the liquid dropout match. A number of possible explanations for that mismatch are possible; we do not know which is the most probable.

Gas 5. Gas 5 exhibits a dewpoint pressure of 4,856.7 psia [33 486 kPa] at 267°F [131°C]. Separation yields 136 bbl [21.6 m^3] of condensate at 440 psia [3034 kPa] and 60°F [16°C] per 1×10^6 scf [28 317 std m^3] of separator gas. Table 1 gives the reservoir fluid composition through C_{7+}. Available data in Table 14 include CCE, CVE, and surface separation data.

A mass balance on the CVE data gave reasonable but slightly erratic liquid gravities as shown on Fig. 9. The regression data set included K-values at the last CVE pressure, surface separation data, CCE data, and values of f_L, γ_g, γ_L, and G_p for each expansion pressure. The erratic 0.6852 liquid gravity at 3,015 psia [20 788 kPa] was omitted from the regression data set.

Fig. 9 compares CVE data with PR and ZJRK results calculated after regression with C_{7+} split into two fractions. Where the circular PR points are not shown, they coincide with the triangular ZJRK points. The agreement with data is very good for both EOS with the exception of z_g and γ_L. Table 15 shows reasonably good agreement between CVE residual liquid compositions using the ZJRK EOS. The PR EOS compositions do not agree as well. Table 16 compares observed and calculated (regressed) EOS results for the two-stage separation. The

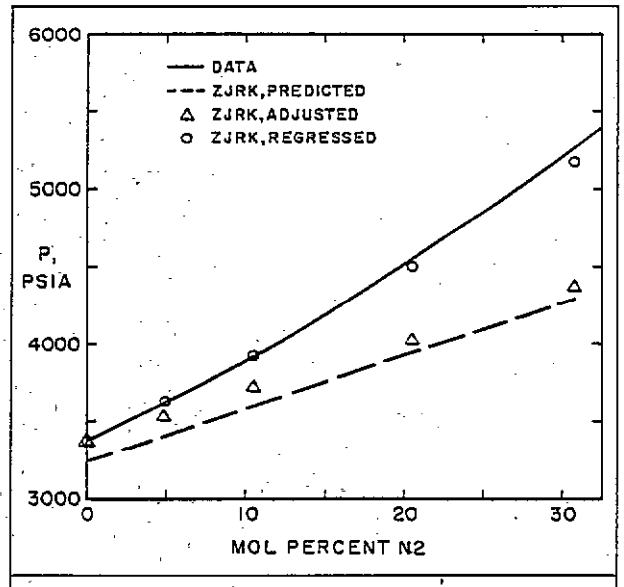

Fig. 6—Gas 4 dewpoint pressure vs. mol% N_2 at 240°F.

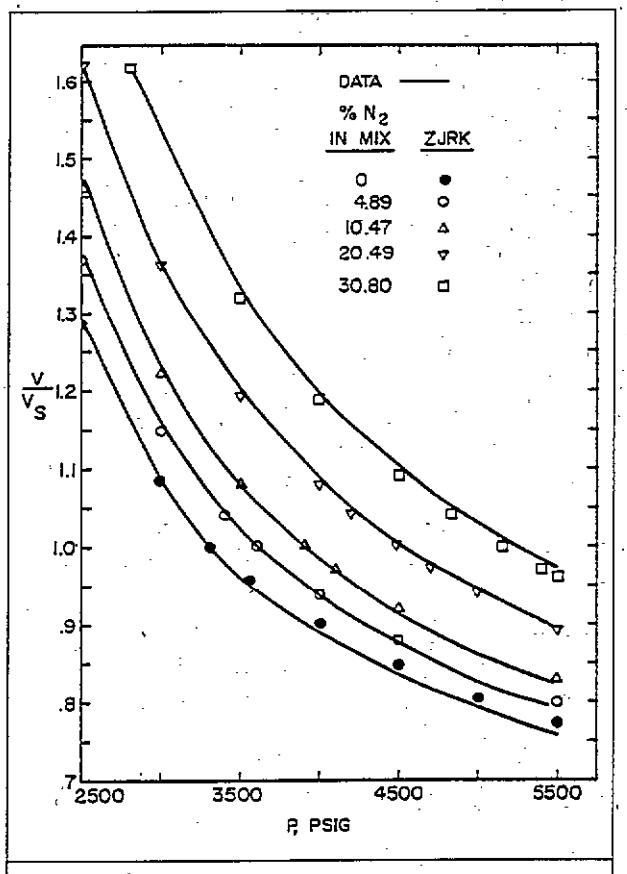

Fig. 7—Gas 4 CCE at 240°F.

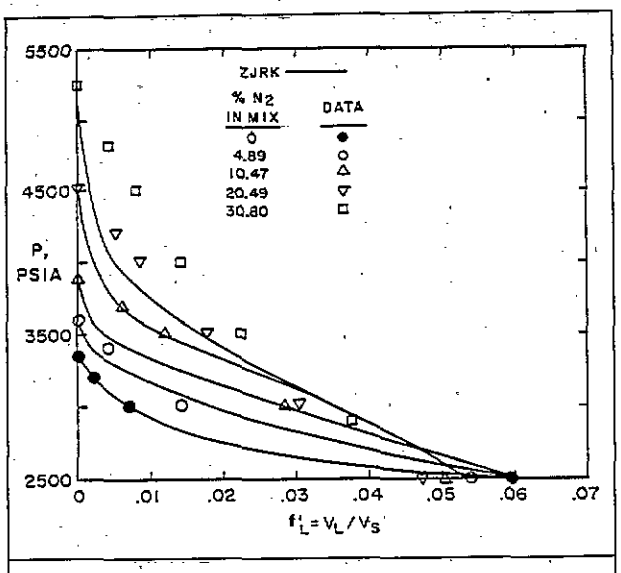

Fig. 8—Gas 4 CCE at 240°F.

GOR is matched exactly, while the calculated stock-tank liquid gravity of 0.805 differs from the observed 0.781.

Oil 1. Oil 1, with composition given in Table 1, has a saturation pressure of 2,535 psia [17 478 kPa] at 180°F [82.2°C]. This fluid was subjected to a multiple-contact vaporization test in which gas with composition given in Table 5 was injected into the oil sample in a visual PVT cell at constant pressure and temperature in a series of steps. At each step, the fluids were allowed to reach an equilibrium. The gas was removed at constant pressure and analyzed. The volume of oil was measured before the next gas injection. This process was continued for 11 injection steps. Measured data from this test are given in Table 5 and include the moles of gas injected and produced, the moles of liquid phase remaining in the cell, the composition of the gas at each injection step, and the composition and molecular weight of the residual oil after the last step of the test. Table 18 compares calculated and observed liquid and gas phase compositions at the last injection step.

The PVT program uses mass-balance considerations to calculate additional data at each step, including oil and gas gravity and liquid-phase molecular weight. The measured molecular weight of the C_{7+} fraction of the gas at the different steps ranged from 105 to 110. The measured oil-phase C_{7+} molecular weights for the reservoir fluid and last-stage fluid were 225 and 258, respectively. This wide range of molecular weight of C_{7+} presented difficulties in matching the vaporization process with only one heavy fraction of molecular weight 225. The vaporized gas at each stage was too heavy, while the residual oil was too light.

A two-component split of the heavy fraction was defined with molecular weights of 147.7 and 318.9, which gave mole fractions of 0.2646 and 0.2178 for Components 9 and 10. This split system gave significantly better results than the nonsplit system as shown in Fig. 10. As Table 11 shows, the regressed, unsplit system gave an average deviation of about 3%. For the split system, the average deviation fell from about 6% after adjustment to 0.31% after regression, exhibiting an excellent match

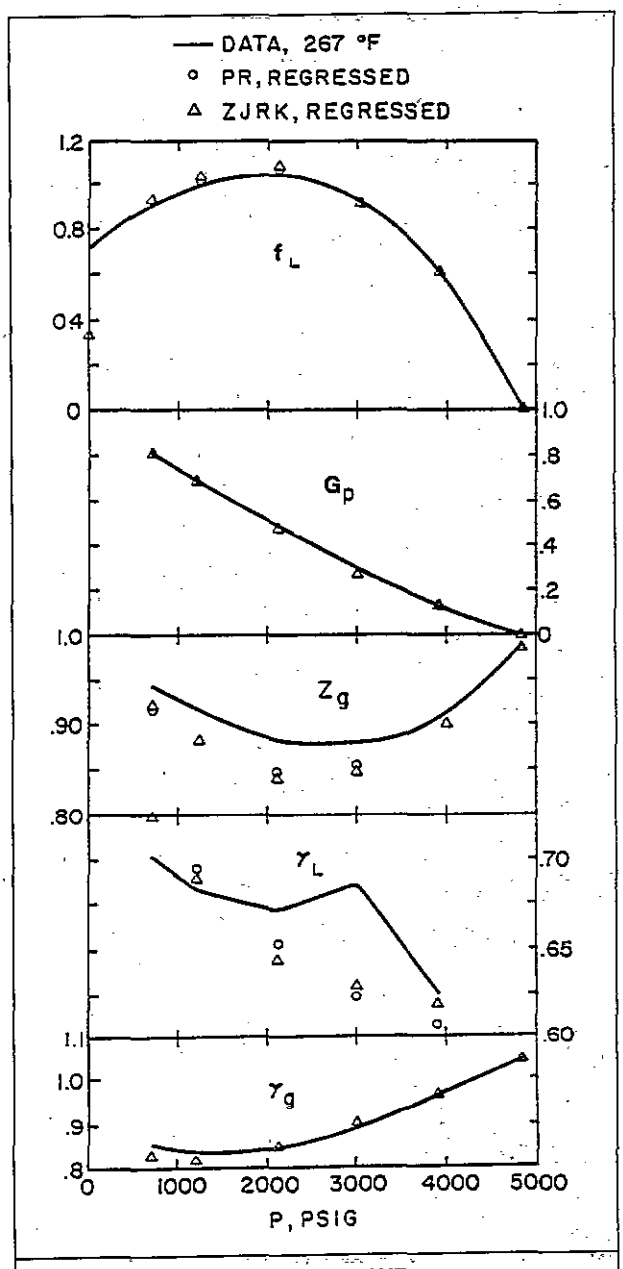

Fig. 9—Gas 5 CVE.

of the data. The regressed results shown in Fig. 10 were obtained by use of the PR EOS with regression on the multiple-contact vaporization data along with CCE data for the reservoir fluid and CCE data for the injection gas. Also shown in Fig. 10 are results obtained by adjusting only the binary in the PR EOS for the two-component split system. Results with the ZJRK EOS were very similar to the PR EOS results.

Oil 2. Oil 2 is very volatile with B_o=2.92, R_s=3,377 at bubblepoint pressure of 4,475 psia [30 854 kPa] and 176°F [80°C]. Two two-stage separations were reported at 60°F [16°C] with 315 and 65 psia [2172 and 448 kPa] primary separator pressures, respectively. The high- and low-pressure separation data gave mass-balance errors of 1.1 and 3.1%, respectively. The laboratory report noted occurrence of waxing in the low-pressure separation. The reservoir-fluid nine-component analysis is reported through a 0.1692 C_{7+} mol fraction with a 173 molecu-

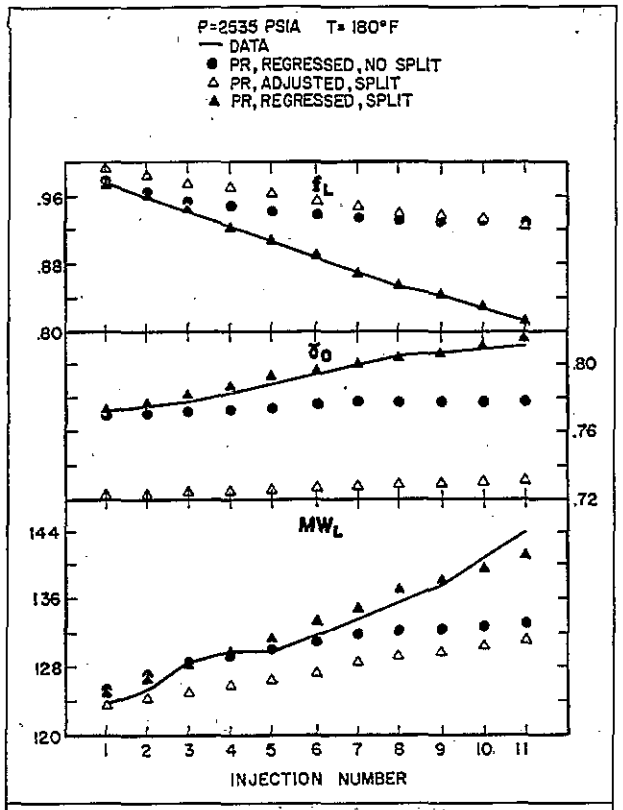

Fig. 10—Oil 1 multiple-contact vaporization test.

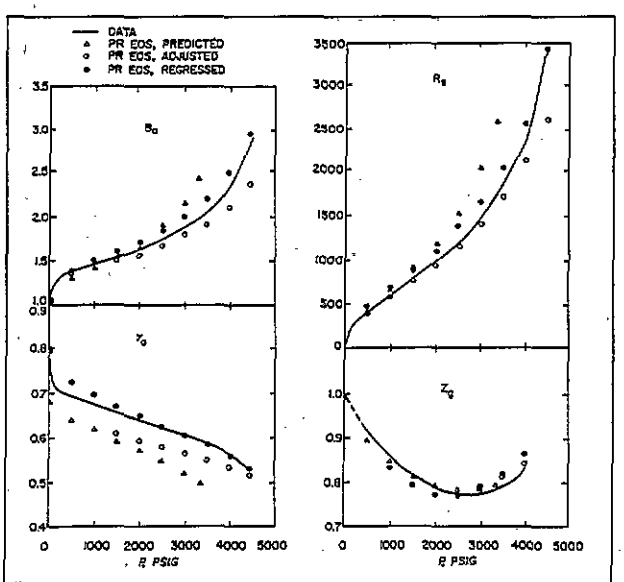

Fig. 11—Oil 2 DE.

lar weight. CCE, CVE, and DE data in Table 6 were used along with all data from the two surface separations in regression.

Both EOS predict bubblepoint pressures of about 3,400 psia [23 442 kPa], considerably below the observed 4,475 psia [30 854 kPa]. With adjustment, both EOS yield B_o and R_s values significantly lower than observed. Table 11 shows that regression reduces the average deviation from 10.25 to 4.68% for the PR EOS. With splitting of the C_{7+} fraction into fractions F_7, F_8, and F_9, and regression on nine variables (Ω_a^c, Ω_b^c of C_1, F_7, F_8, F_9,

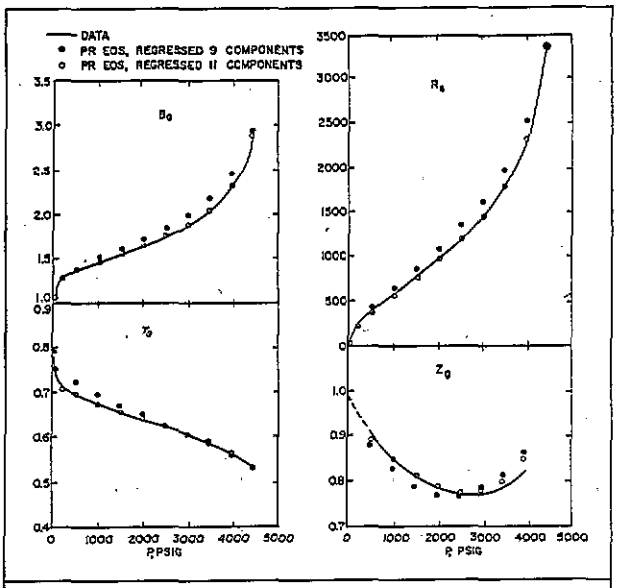

Fig. 12—Oil 2 DE.

and the C_1/F_9 binary), the average deviation falls further to 2.17%.

Figs. 11 and 12 compare DE observed and calculated B_o, R_s, and liquid gravity for the PR EOS for the cases of prediction, adjustment, and regression. Fig. 12 shows that the C_{7+} splitting with regression results in a virtually exact match of the DE data.

None of the regressions with either EOS gave good matches of the surface separation data, as shown in Table 12. Regression with the surface separation data alone also resulted in a poor match with either EOS. This, combined with the mass-balance error in the data and occurrence of waxing, lead us to suspect the data.

Oil 3. Oil 3 contains 60 mol% CO_2 and exhibits a bubblepoint of 2,612 psia [18 010 kPa] at the reservoir temperature of 179°F [82°C]. CCE data for this sample at temperatures ranging from 140 to 200°F [60 to 93°C] are shown in Table 7. The reported analysis to C_{10+} for this sample is given in Table 1. Fig. 13 shows the match of saturation pressure with the PR EOS with 12 components over the range of temperatures. Predicted values are approximately 500 psi [3447 kPa] lower than experimental values. Adjustment gives good agreement, while regressed results virtually duplicate the experimental data. CCE results are shown in Fig. 14. The PR EOS-predicted values give large error for both relative volume and liquid volume. Regressed results agree well with the data.

As indicated by the average deviations in Table 11, the regressed PR results match the data significantly better than the regressed ZJRK results. However, use of only nine components (through C_{7+}), with either EOS, gives agreement with data almost equal to that obtained with 12 components through C_{10+}.

The regression data set included CCE data at the four temperatures. The usual five-parameter regression varible set was used except that CO_2 replaced methane.

Oil 4. Oil 4 is slightly volatile with B_o=1.671 and R_s=932 at 250°F [121°C]. The nine-component analy-

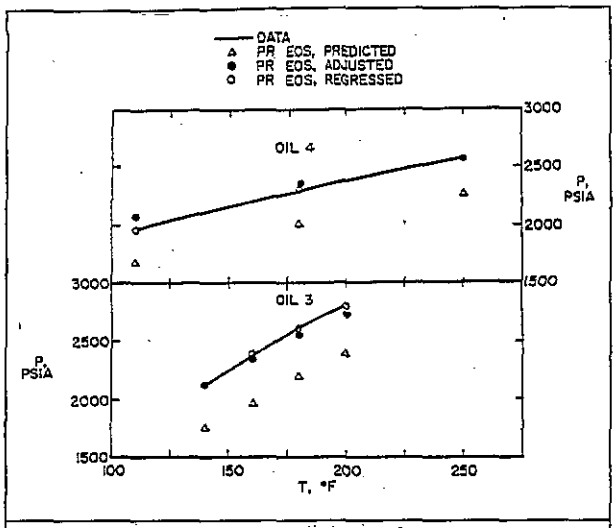

Fig. 13—Effect of temperature on saturation pressure.

sis of this sample through C_{7+} is shown in Table 1, with CCE, DE, and separation data given in Table 8. The effect of temperature on saturation pressure is shown for Oil 4 in Fig. 13. The PR EOS-predicted values for saturation pressure are in error as much as 500 psi [3447 kPa]. Adjustment improves the calculation, but regression again virtually duplicates these data. Results from a DE of Oil 4 at 110°F [43°C] are given in Fig. 15. The adjusted PR results are very low for R_s, B_o, and γ_o, with the γ_o values showing the most error. Regression provides an excellent match of all data for this sample.

Splitting the C_{7+} resulted in insignificant improvement in agreement between observed and regressed EOS results. The average deviations of 2.3 to 2.6% after regression shown in Table 11 indicate that the two EOS give comparable agreement with data. The regression data set included all CCE and DE expansions and all surface separation data.

Oil 5. All data used for Oil 5 are given by Hoffmann *et al.*[17] Their data include extended analyses through F_{22} for a saturated oil and its associated gas. Data are given for flash of the oil at 14.7 psia [101 kPa] and 60°F [16°C], flash of the associated gas at 800 psia [5516 kPa] and 83°F [28°C], and CCE data at 201°F [94°C] for the associated gas.

Katz and Firoozabadi[1] applied the PR EOS to these data. They concluded that the EOS accurately predicted the associated gas data and, with adjustment, matched the oil data. In part, their conclusion rested on close agreement between the observed gas composition and that calculated from the oil composition by use of the adjusted EOS.

Practical considerations in simulation require that a single set of EOS parameters be used to represent both the oil leg and gas cap in a saturated reservoir. Calculations here therefore use only the oil composition as known input data. All calculations of the gas CCE and flash use the *calculated* composition of gas in equilibrium with the oil at calculated bubblepoint pressure and 201°F [94°C].

Figs. 16 and 17 compare observed and calculated liquid dropout and gravity from a CCE of the associated gas sample for Oil 5. Adjusted values for a 22-component system and regressed values for a seven-component system

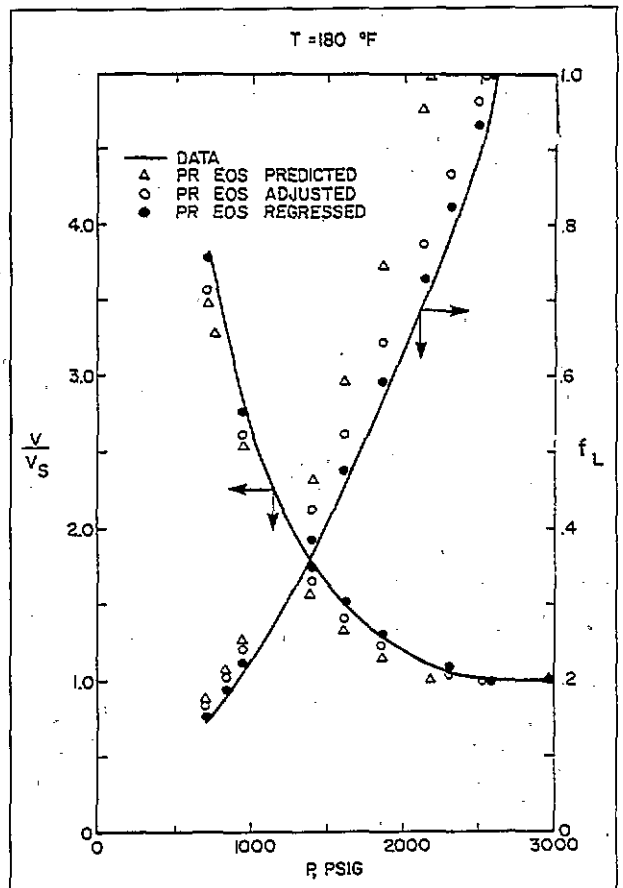

Fig. 14—Oil 3 CCE.

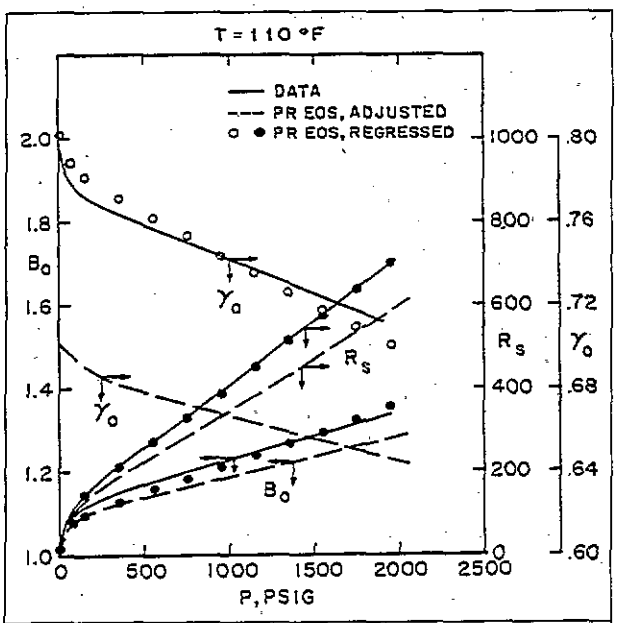

Fig. 15—Oil 4 DE.

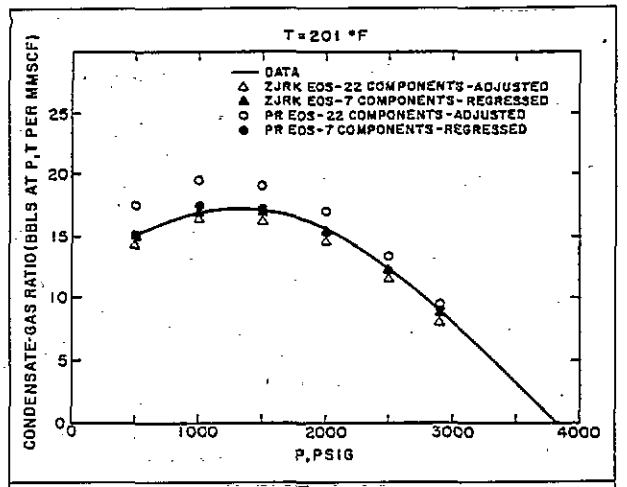

Fig. 16—CCE of Oil 5 associated gas.

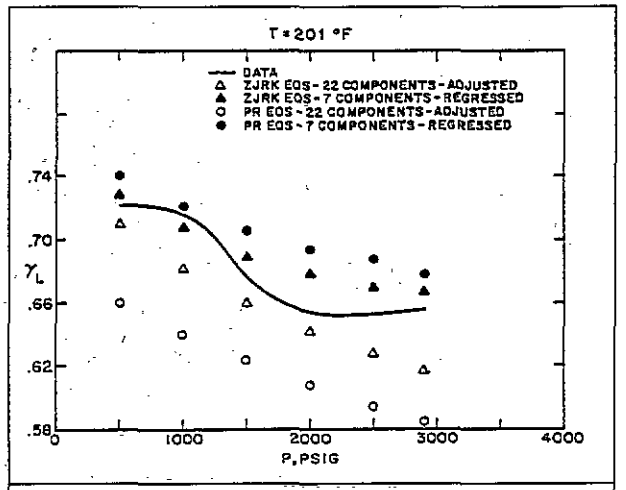

Fig. 17—Gravity of separator liquid, CCE of associated gas from Oil 5.

using both the PR and ZJRK EOS are presented. The adjusted 22-component EOS results compare reasonably well with data; the regressed seven-component results compare significantly better and about equally well for both EOS. Table 11 shows that for both EOS, seven-component regressions give average deviations of about 2%, as low as or lower than 22-component regressions. With 22 components and the usual five regression variables, nonconvergence occurred. Removal of the binary from the variable set resulted in convergence.

Both EOS's predicted bubblepoint pressures about 500 psia [3447 kPa] too low with either 7 or 22 components. The gas flash results in Table 12 show that the use of 22 rather than 7 components results in more accurate EOS-predicted and adjusted values of the flashed-gas GOR. The seven-component regressed EOS result, however, compares well with this GOR.

Oil 6. Oil 6 is moderately volatile with $B_o = 1.866$ and $R_s = 1{,}230$ at 234°F [112°C]. The nine-component analysis includes minor amounts of CO_2 and N_2 and a 0.3043 C_{7+} fraction with a molecular weight of 200. The CCE and DE data, along with data from four two-stage separations at 74°F [23°C], given in Table 9, were used

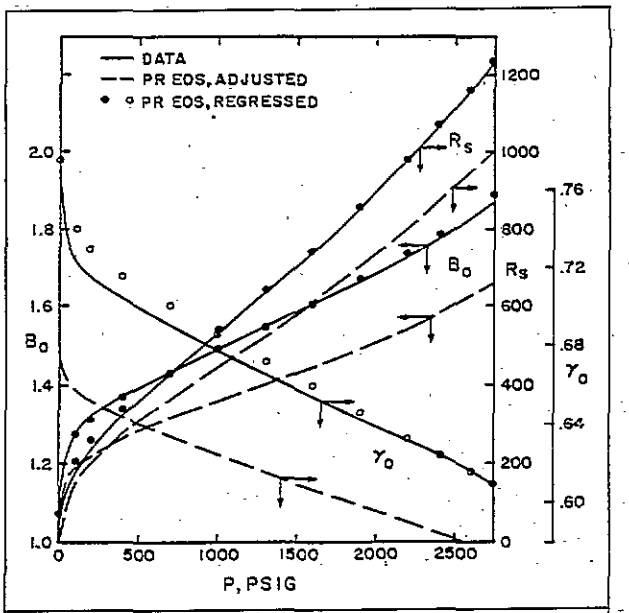

Fig. 18—Oil 6 DE.

in regression. Table 11 shows that regression resulted in average deviations of 2.1 and 2.67% for the PR and ZJRK EOS, respectively. Fig. 18 and Table 12 show the close match of data after regression with the PR EOS. Splitting gave insignificant improvement.

Oil 7. Oil 7 is the least volatile of the oil samples with $B_o = 1.324$ and $R_s = 557$ at 131°F [55°C]. The CCE and DE data along with data from four two-stage surface separations at 72°F [22°C] given in Table 10 were used in regression. The nine-component analysis includes minor amounts of CO_2, N_2, and a 0.3597 C_{7+} mol fraction with a molecular weight of 252. Table 11 shows that both EOS give average deviations of about 4% after regression. With adjustment only, the ZJRK EOS gives a significantly better fit of the data. Splitting the C_{7+} fraction into three fractions gave insignificant improvement in the match of data.

Conclusions

Among the PVT program features described, we find the regression capability most important in efficient validation of an EOS before its use in a compositional simulator.

Data given for six oil and three retrograde gas condensate samples include constant-composition, constant-volume, and differential expansions, surface separations, temperature-dependent saturation pressures, and N_2 reservoir fluid behavior. One set of multiple-contact oil vaporization data is reported.

The PR and ZJRK EOS are applied to these nine fluids and three published fluid data sets under conditions of prediction (no alteration of EOS parameters), adjustment (altering one binary coefficient), and regression. Agreement between laboratory data and regressed EOS results is generally good to excellent. Results for these 12 fluids and a larger number of unreported studies indicate that regressed PR and ZJRK EOS give very comparable agreement with data.

In either predictive or adjusted modes, both EOS give generally poor agreement with any reasonably complete

set of laboratory PVT data. We find regression necessary for required engineering accuracy in EOS results.

Our studies indicate that regression on the methane/plus-fraction Ω_a°, Ω_b° EOS parameters and the methane-plus fraction binary is frequently necessary and sufficient for good data matches. Further, we find a minimal need for the extensive splitting of C_{7+} used to match data in several published studies. In this work, generally good agreement with data was obtained with C_{7+} splits ranging from none to four fractions.

The extent of splitting required depends primarily on the recovery process anticipated. Below-dewpoint cycling of condensate reservoirs and gas (or CO_2, N_2) injection into oil or gas reservoirs give rise to vaporization effects requiring some C_{7+} splitting. Depletion and/or waterflooding operations, even in near-critical condensate or highly volatile oil reservoirs, may frequently be simulated compositionally with little or no splitting of the C_{7+} fraction.

The results of this work illustrate our general observation that an EOS tuned by comparison with only reservoir-temperature (e.g., expansion) PVT data frequently gives good agreement with surface separation data.

In some cases, such as Oil 2 and Gas 4 of this study, a portion of laboratory PVT data may remain poorly matched by regressed EOS results. Such disparity can frequently be resolved by more fully exploring regression variable sets and C_{7+} characterization (splitting). Remaining disparity leaves an open question regarding causes of EOS inadequacy as opposed to poor data. Data errors and inconsistencies can be detected in some cases by simple mass-balance calculational checks.

Nomenclature

B_o = oil FVF obtained from a differential expansion, RB/STB [res m^3/stock-tank m^3]
B_{oF} = oil FVF obtained by surface separation, RB/STB [res m^3/stock-tank m^3]
b, b_{j+} = methane-plus fraction binary interaction coefficient
b_{ij} = binary interaction coefficient between components i and j
$\hat{b}$ = value of b determined in EOS adjustment
d_j = observation (data item) j included in a regression data set
d_{jC} = calculated value of d_j
f_L = volume fraction liquid in expansion cell, V_L/V
f'_L = volume fraction liquid in expansion cell, V_L/V_S
F = objective function, defined in Eq. 1
F^* = value of F on convergence of regression
G_p = volume or mole fraction of gas removed from a laboratory constant-volume expansion cell
$M+$ = molecular weight of the plus fraction
n_C = number of components
n_J = total number of observations in regression data set
p = pressure, psia [kPa]
p_c = critical pressure, psia [kPa]
R_s = solution gas obtained from a differential expansion, scf/STB [std m^3/stock-tank m^3]
R_{sF} = solution gas obtained from a surface separation, scf/STB [std m^3/stock-tank m^3]
T = temperature, °F [°C]
T_c = critical temperature, °R [K]
v_i = regression variable i
V = laboratory expansion cell total volume
V_L = volume of liquid in expansion cell
V_S = volume of expansion cell at saturation pressure
W_i = weight factor on observation d_i in definition of regression objective function, F
z = gas-phase deviation factor
γ_g = gas gravity, air=1.0
γ_L = hydrocarbon liquid gravity, water =1.0
γ_o = oil gravity, water=1.0
ϵ = average deviation, F^*/n_J
ρ_s = density of fluid at saturation pressure and reservoir or test temperature, lbm/cu ft [kg/m^3]
$\Omega_{ai}^\circ, \Omega_{bi}^\circ$ = cubic EOS parameters for Component i

Subscripts

c = critical
C = calculated, component
F = surface separation or flash
g = gas
i, j = component number
L = hydrocarbon liquid
o = oil

References

1. Katz, D.L. and Firoozabadi, A.: "Predicting Phase Behavior of Condensate/Crude-Oil Systems Using Methane Interaction Coefficients," *J. Pet. Tech.* (Nov. 1978) 1649–55; *Trans.*, AIME, **265**.
2. Firoozabadi, A., Hekim, Y., and Katz, D.L.: "Reservoir Depletion Calculations for Gas Condensates Using Extended Analyses in the Peng-Robinson Equation of State," *Cdn. J. Chem. Eng.* (1978) **56**, 610–15.
3. Yarborough, Lyman: "Application of a Generalized Equation of State to Petroleum Reservoir Fluids," *Equations of State in Engineering*, Advances in Chemistry Series, K.C. Chao and R.L. Robinson (eds.), American Chemical Society, Washington, DC (1979) **182**, 385–435.
4. Baker, L.E. and Luks, K.D.: "Critical Point and Saturation Pressure Calculations for Multicomponent Systems," *Soc. Pet. Eng. J.* (Feb. 1980) 15–24.
5. Vogel, J.L. and Yarborough, L.: "The Effect of Nitrogen on the Phase Behavior and Physical Properties of Reservoir Fluids," paper SPE 8815 presented at the 1980 SPE/DOE Enhanced Oil Recovery Symposium, Tulsa, April 20–23.
6. Whitson, C.H.: "Characterizing Hydrocarbon Plus Fractions," *Soc. Pet. Eng. J.* (Aug. 1983) 683–94.
7. Whitson, C.H. and Torp, S.B.: "Evaluating Constant-Volume Depletion Data," *J. Pet. Tech.* (Mar. 1983) 610–20.
8. Peneloux, A., Jain, C., and Behar, E.: "Application of the Developed Redlich-Kwong Equation of State to Predict the Thermodynamic Properties of Condensate Gases," paper SPE 8287 presented at the 1979 SPE Annual Technical Conference and Exhibition, Las Vegas, Sept. 23–26.

9. Williams, C.A., Zana, E.N., and Humphrys, G.E.: "Use of the Peng-Robinson Equation of State to Predict Hydrocarbon Phase Behavior and Miscibility for Fluid Displacement," paper SPE 8817 presented at the 1980 SPE/DOE Enhanced Oil Recovery Symposium, Tulsa, April 20-23.
10. Coats, K.H.: "Simulation of Gas Condensate Reservoir Performance," *J. Pet. Tech.* (Oct. 1985) 1870-86.
11. Redlich, O. and Kwong, J.N.S.: "On the Thermodynamics of Solution V. An Equation of State. Fugacities of Gaseous Solution," *Chem. Review* (1949) **44**, 233.
12. Soave, G.: "Equilibrium Constants From a Modified Redlich-Kwong Equation of State," *Chem. Eng. Sci.*, (1972) **27**, 1197-1203.
13. Zudkevitch, D. and Joffe, J.: "Correlation and Predictions of Vapor-Liquid Equilibria with the Redlich-Kwong Equation of State," *AIChE J.* (Jan. 1970) **16**, 112-19.
14. Joffe, J., Schroeder, G.M., and Zudkevitch, D.: "Vapor-Liquid Equilibria with the Redlich-Kwong Equation of State," *AIChE J.* (May 1970) **16**, 496-98.
15. Peng, D.-Y. and Robinson, D.B.: "A New Two-Constant Equation of State," *Ind. Eng. Chem. Fundam.* (1976) **15**, 59.
16. Lohrenz, J., Bray, B.G., and Clark, C.R.: "Calculating Viscosities of Reservoir Fluids From their Compositions," *J. Pet. Tech.* (Oct. 1964) 1171-76; *Trans.*, AIME, **231**.
17. Hoffmann, A.E., Crump, J.S., and Hocott, C.R.: "Equilibrium Constants for a Gas-Condensate System," *J. Pet. Tech.* (Jan. 1953) 1-10; *Trans.*, AIME, **198**.
18. Coats, K.H., Dempsey, J.R., and Henderson, J.H.: "A New Technique for Determining Reservoir Description from Field Performance Data," *Soc. Pet. Eng. J.* (March 1970) 66-74.
19. Coats, K.H.: "Reservoir Simulation: State of the Art," *J. Pet. Tech.* (Aug. 1982) 1633-42.

Appendix—Selection and Range Limits of Regression Variables

Our experience with EOS regression includes a wide variety of fluid samples and types of laboratory test data. In general, a necessary and sufficient regression variable set has been the five parameters of methane and plus-fraction Ω's and methane-plus fraction binary.

When a CO_2 swelling test is part of the data, we usually find it necessary to add CO_2 Ω_b° to the variable set and pure CO_2 density (at reservoir temperature and a pertinent pressure) to the data set. The further addition of the CO_2-plus fraction binary may or may not prove helpful. For N_2/reservoir fluid mix data, we have found the basic five-parameter variable set sufficient with no alteration or inclusion of N_2 EOS parameters. However, we have more experience with CO_2 reservoir fluid data than with N_2 mix data.

One obvious rule in selecting regression variables is exclusion of any EOS parameter that, by inspection, cannot affect significantly the calculated value of any of the regression data. For example, if compositions of all samples in a regression data set include very small amounts of some component, then one would not select any of that component's Ω's or binaries as regression variables. The pragmatic converse of this rule is inclusion of one or more EOS parameters for any component that is compositionally predominant in all or some regression data samples. In many cases, methane satisfies this predominance.

TABLE A-1—EFFECT OF PSEUDOIZATION ON C_{7+} Ω_{a+}°, Ω_{b+}°

Oil	EOS	Ω_{a+}°	Ω_{b+}°
5	PR	0.5296	0.0872
5	ZJRK	0.3935	0.0854
3	PR	0.5183	0.0858
3	ZJRK	0.3874	0.0848

The characteristics of a good or optimal regression variable set are that the regression converges; the variable values converged upon are realistic; deletion of any member of the variable set results in either or both of (1) a significantly worse data match and (2) unrealistic variable values; and addition of any other EOS parameter results in either or both of (1) nonconvergence and (2) insignificantly better data match.

Nonconvergence can result from redundancy among the variables in the sense that the objective function is insensitive to values of two or more variables provided they satisfy some relationship to one another. Nonconvergence can also result from simple insensitivity of the objective function to one or more of the variables. The symptom of nonconvergence may be either the tailing off toward global limit or the "bouncing" within a small range of one or more of the variables.

In any event, nonconvergence is obviously dependent on the regression data set as well as the variable set. That is, a given variable set yielding nonconvergence may yield quite reasonable convergence with additional regression data. For a fixed regression data set, the remedy for nonconvergence is simply removal of one of the regression variables. The response to a convergence with unrealistic variable values should be addition of a regression variable, as illustrated in the case of Gas 3 of this paper.

The occurrence of a poor data match with a regression variable set that obeys the previously mentioned characteristics of a good regression variable set, with or without realistic convergence, indicates either erroneous data or inadequacy of the EOS. In some cases, suspect data can be detected by simple mass balances on CVE data and/or surface separation results. In one lean retrograde-gas-condensate case, the laboratory data included liquid dropout V_L/V values for a CCE about three times larger than the CVE V_L/V_S values. All "good" gas-condensate data we have seen exhibit CVE f_L values larger than CCE f_L values. A mass balance on that particular condensate's CVE gave liquid gravities ranging from 22 near dewpoint to 18 at lower pressure. Omission of the CVE f_L values from the regression data set gave quite reasonable EOS parameter values and a good data match, except that calculated (more correct) CVE f_L values were about five times larger than reported.

The above discussion gives no rationalization for accepting or allowing alteration of EOS parameter theoretical values. The theoretical Ω_a° and Ω_b° values in cubic EOS arise from the required satisfaction of the van der Waals conditions of $dp/dV = d^2p/dV^2 = 0$ at the critical point. The component temperature functions in the SRK and PR EOS and the altered (temperature-dependent) ZJRK component Ω° values essentially reflect satisfaction of pure-component density and vapor-pressure data below critical temperature. At reservoir conditions, methane in particular is well above its critical point and there is no theory or clear-cut guide to selection or alteration of Ω's for components well above their critical temperature. One might argue pragmatically that the theoretical methane Ω_a° and Ω_b° values satisfying the van der Waals conditions at p and T far removed from our range of interest do not satisfy the requirement of correct methane density at the reservoir p and T conditions that are of interest. Pursuing this observation leads to the suggestion that methane Ω_a°, Ω_b° be determined at reservoir

temperature by requiring exact satisfaction of methane densities at that temperature and two pertinent pressures. A next step is pinning only the relationship between the two Ω's by satisfying experimental density at one pressure and regressing on one Ω. We have done this with the CO_2 Ω's in connection with a swelling test match[19] and found that the resulting CO_2 Ω_a° and Ω_b° values yielded excellent agreement with pure CO_2 density over a wide range of pressures.

Arguments in favor of accepting altered plus-fraction Ω° values basically reflect the simple fact that, unlike all other components, that fraction is a mixture of many components. One argument for accepting altered values of Ω_{a+}°, Ω_{b+}° can be based on the results of pseudoizing or lumping an extended analysis to a C_{7+} fraction. A pseudoization procedure[10] was applied to the Oil 5 and Oil 3 extended analyses. The Oil 5 F_7 through F_{22+} fractions and Oil 3 C_7 through C_{10+} fractions were each lumped into single C_{7+} fractions, using both EOS. Table 18 lists the resulting C_{7+} Ω_a° and Ω_b° values.

SI Metric Conversion Factors

°API	141.5/(131.5+°API)		= g/cm³
bbl	× 1.589 873	E−01	= m³
cp	× 1.0*	E−03	= Pa·s
cu ft	× 2.831 685	E−02	= m³
cu in.	× 1.638 706	E+01	= cm³
°F	(°F−32)/1.8		= °C
lbm/cu ft	× 1.601 846	E+01	= kg/m³
psi	× 6.894 757	E+00	= kPa
scf/STB	× 1.781 073	E−01	= std m³/ stock-tank m³

*Conversion factor is exact.

SPERE

Original manuscript received in the Society of Petroleum Engineers office Aug. 27, 1982. Paper accepted for publication Feb. 9, 1983. Revised manuscript received Aug. 5, 1985. Paper (SPE 11197) first presented at the 1982 Annual Fall Technical Conference and Exhibition held in New Orleans, Sept. 26–29.

TABLE 17
EXPANSION AND SEPARATION DATA FOR OIL 6

DIFFERENTIAL EXPANSION AT 234° F.

Pressure, PSIG	Relative Oil Volume	Solution Gas/Oil Ratio	Deviation Factor Z	Oil Density, Gm/cc	Gas Gravity
2746*	1.866	1230		0.6090	
2598	1.821	1151	0.852	0.6162	0.848
2400	1.771	1059	0.849	0.6240	0.849
2200	1.725	972	0.851	0.6314	0.841
1897	1.658	849	0.858	0.6433	0.836
1600	1.599	737	0.870	0.6543	0.837
1300	1.543	631	0.885	0.6655	0.846
1000	1.488	529	0.906	0.6767	0.872
700	1.433	428	0.925	0.6888	0.920
394	1.371	321	0.951	0.7028	1.038
195	1.313	231		0.7145	1.248
112	1.274	178		0.7231	1.458
0	1.086	0		0.7667	2.245

CCE AT 234° F.

p, PSIG	V/V_s
5000	0.9581
4500	0.9655
4000	0.9738
3500	0.9829
3200	0.9892
3100	0.9915
3000	0.9937
2900	0.9961
2800	0.9986
2746*	1.0000
2734	1.0023
2721	1.0042
2692	1.0090
2605	1.0218
2500	1.0410
2362	1.0697
2203	1.1082
2012	1.1661
1815	1.2432
1608	1.3497
1415	1.4853
1225	1.6697
968	2.0395
742	2.6216
535	3.5732

SEPARATOR TESTS

p, PSIG	T, °F.	Separator GOR	Stock Tank GOR	Stock Tank Gravity °API @ 60° F.	Formation Volume Factor	Specific Gravity of Separator Gas
0	74	1059		40.9	1.722	0.996
50	74	874	53	42.4	1.627	
100	74	810	100	42.7	1.610	
200	74	722	188	42.6	1.611	

* Bubble point pressure

TABLE 18
EXPANSION AND SEPARATION DATA FOR OIL 7

DIFFERENTIAL EXPANSION AT 131° F.

Pressure PSIG	Relative Oil Volume	Solution Gas/Oil Ratio	Deviation Factor Z	Oil Density Gm/cc	Gas Gravity
1694*	1.324	557		0.7126	
1550	1.311	526	0.718	0.7157	0.854
1400	1.298	493	0.717	0.7190	0.860
1252	1.285	460	0.716	0.7223	0.869
1100	1.270	423	0.716	0.7265	0.880
950	1.256	389	0.718	0.7300	0.889
798	1.240	349	0.726	0.7345	0.905
643	1.224	310	0.736	0.7392	0.914
500	1.209	273	0.755	0.7434	0.927
350	1.188	229	0.806	0.7498	0.940
200	1.160	179	0.918	0.7594	0.958
102	1.136	137	1.117	0.7663	
0	1.034	0	1.513	0.7981	

CCE AT 131° F.

p, PSIG	V/V_s
5000	0.9707
4500	0.9743
4000	0.9784
3500	0.9825
3000	0.9871
2500	0.9917
2100	0.9957
2000	0.9968
1900	0.9978
1800	0.9989
1700	0.9999
1694*	1.0000
1682	1.0026
1670	1.0048
1642	1.0100
1572	1.0242
1475	1.0477
1377	1.0764
1263	1.1163
1128	1.1614
1000	1.2098
870	1.3016
750	1.3298
588	1.8573
462	2.2664
352	2.9035
258	3.9479

SEPARATOR TESTS

p, PSIG	T, °F.	Separator GOR	Stock Tank GOR	Stock Tank Gravity °API @ 60° F.	Formation Volume Factor	Specific Gravity of Separator Gas
0	72	580		39.7	1.340	1.075
40	72	472	43	41.5	1.306	
80	72	424	80	41.6	1.299	
160	72	366	142	41.5	1.302	

* Bubble point pressure

FIGURE 1

GAS 1 CONSTANT VOLUME EXPANSION 180.5 °F

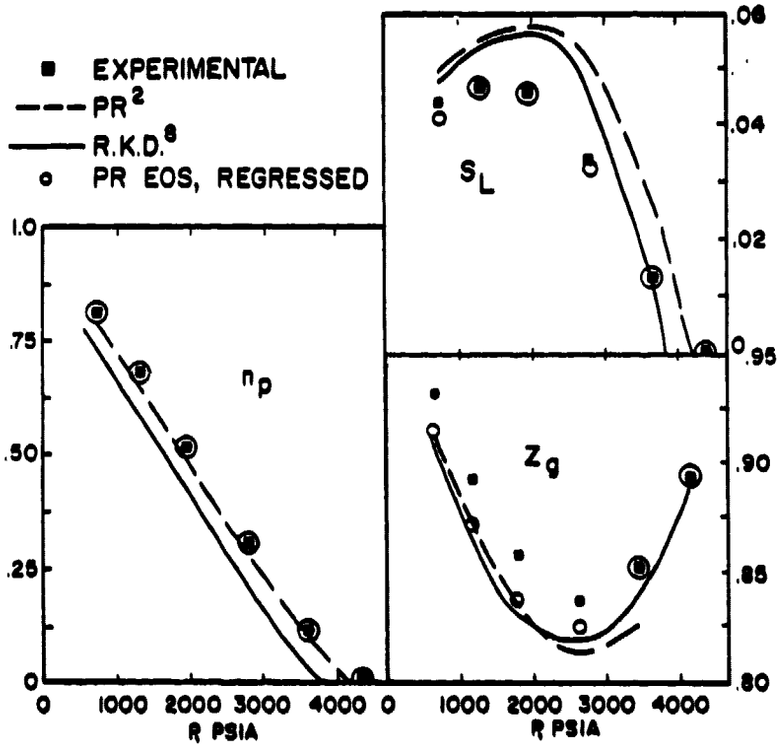

FIGURE 2

GAS 2 CONSTANT COMPOSITION EXPANSIONS

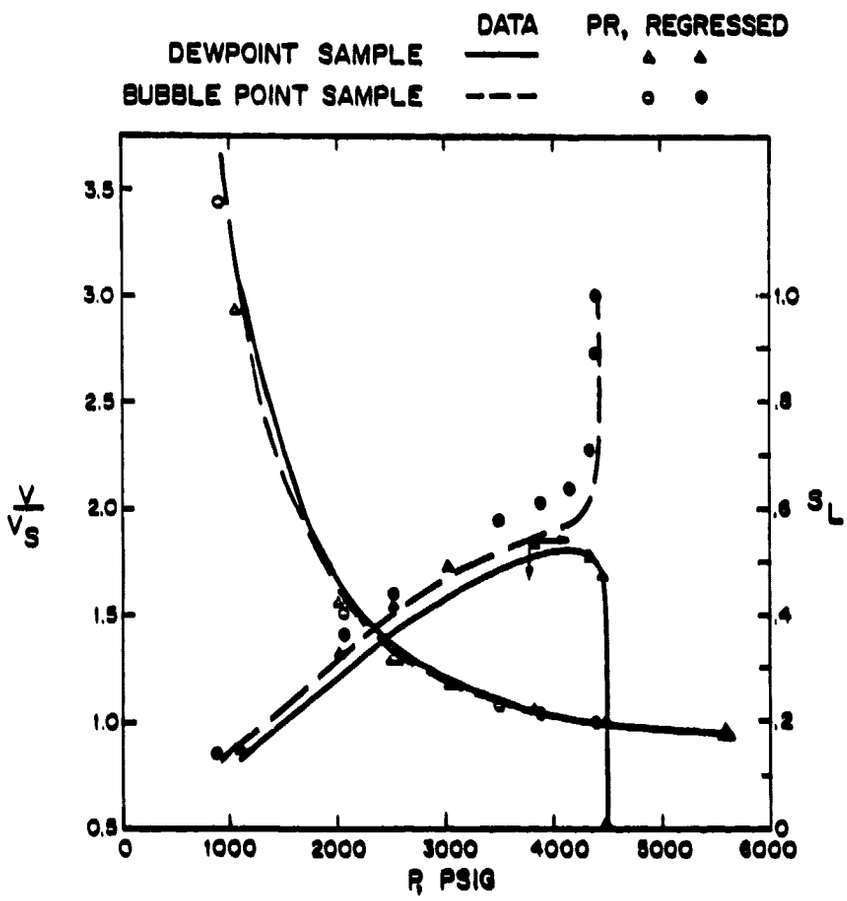

FIGURE 3

GAS 2 CONSTANT VOLUME EXPANSION

DEWPOINT SAMPLE, 190 °F

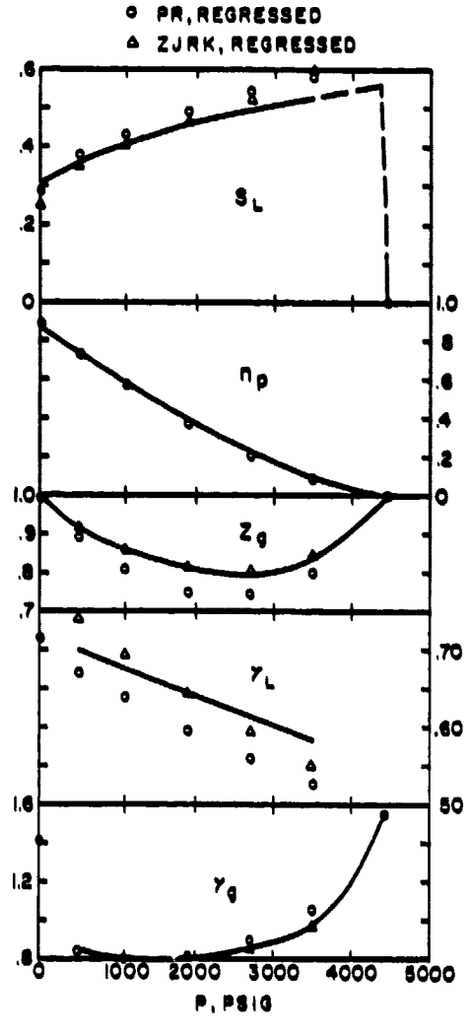

FIGURE 4

GAS 3 -N2 MIX CCE

225.8 °F

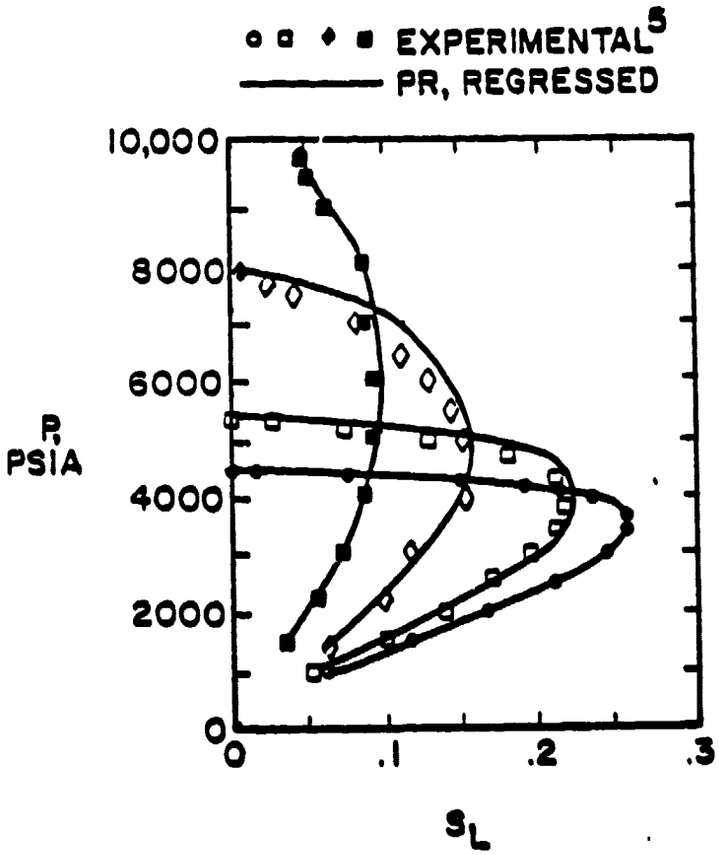

FIGURE 5

GAS 4 DEWPOINT PRESSURE VS. TEMPERATURE

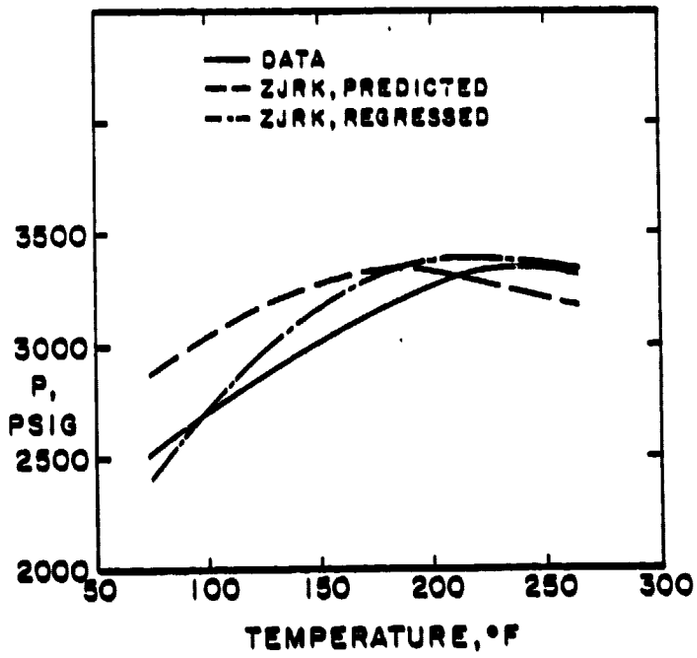

FIGURE 6

GAS 4 DEWPOINT PRESSURE VS. MOL PERCENT NITROGEN, 240 °F

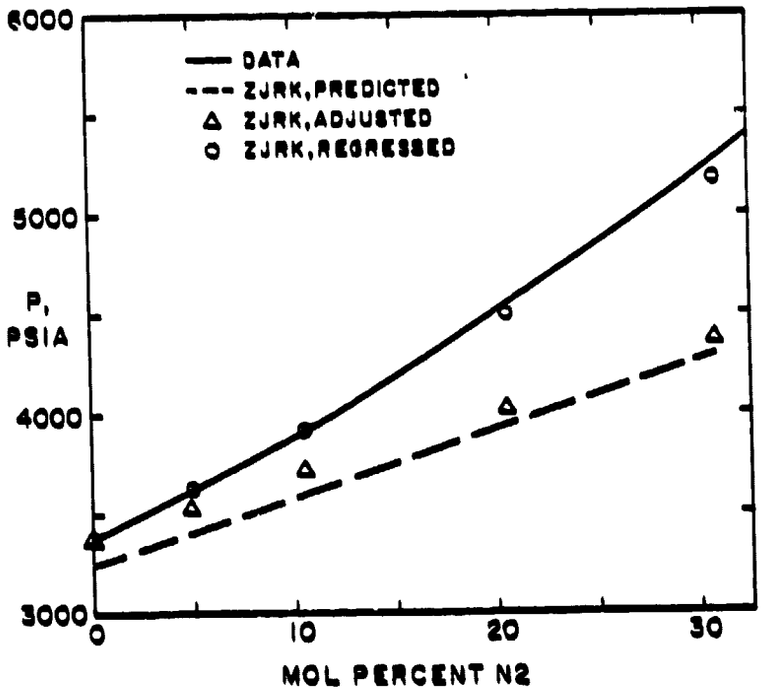

FIGURE 7

GAS 4 CONSTANT COMPOSITION EXPANSION

240 °F

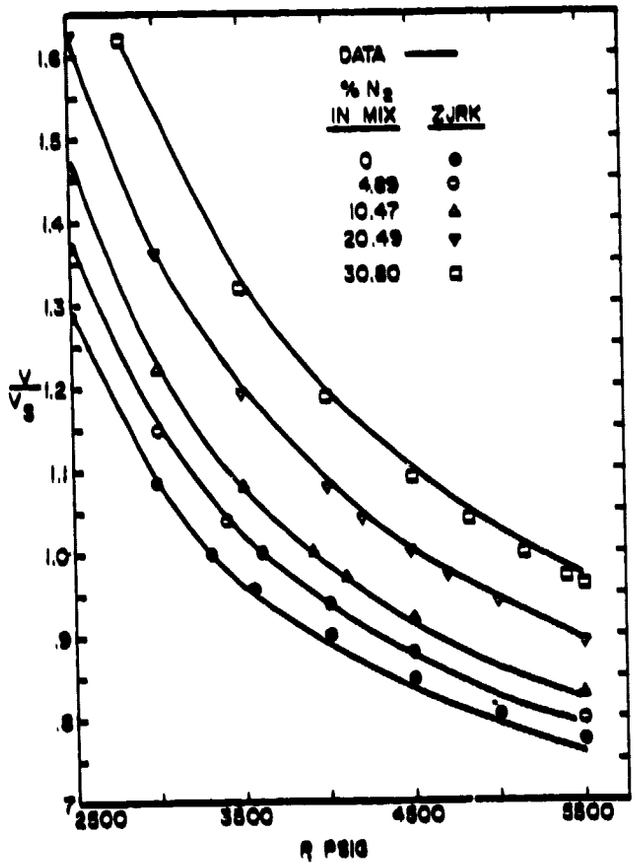

FIGURE 8

GAS 4 CONSTANT COMPOSITION EXPANSIONS, 240 °F

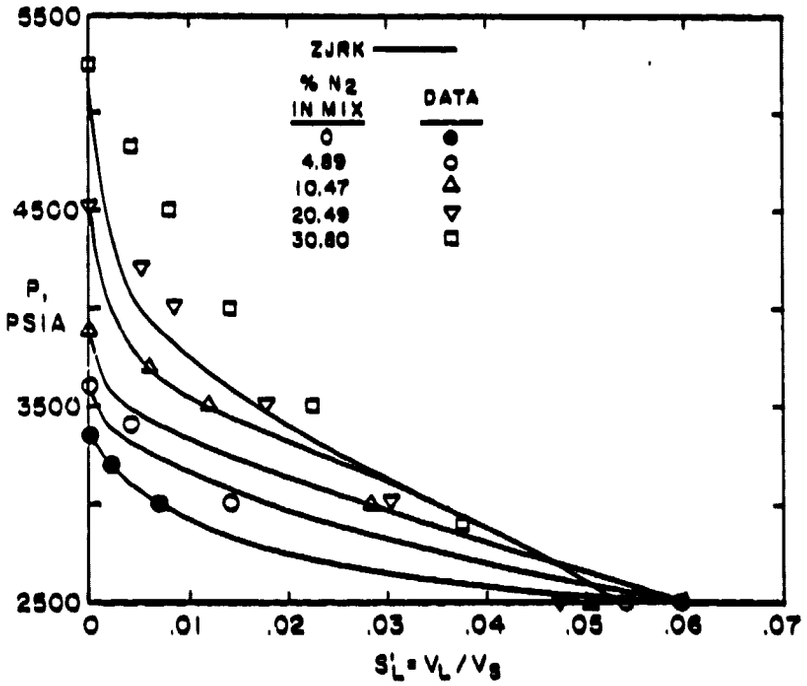

FIGURE 9

GAS 5 CONSTANT VOLUME EXPANSION

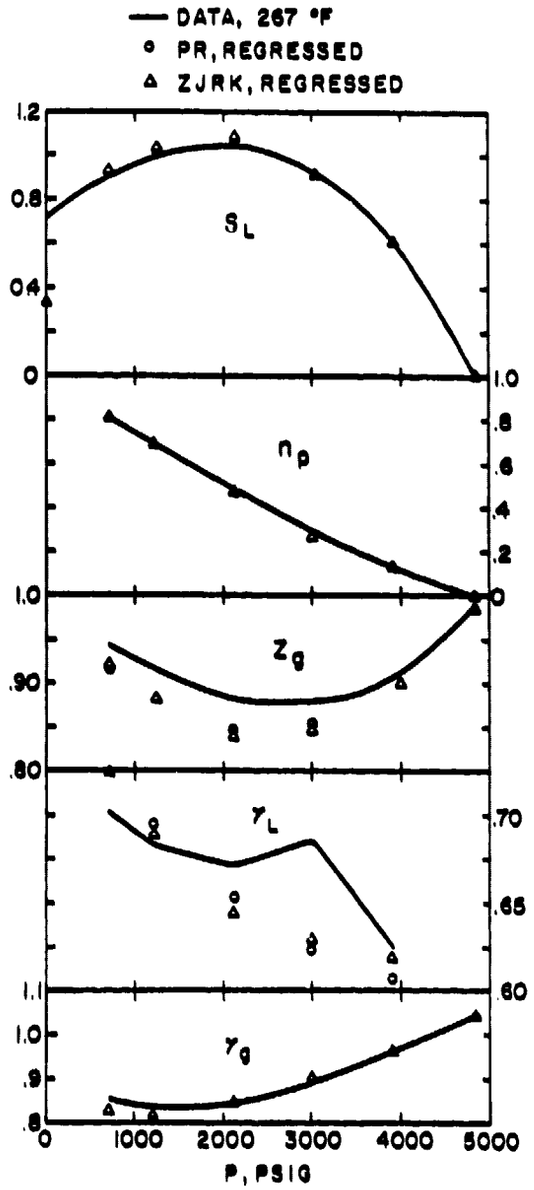

FIGURE 10

OIL 1 MULTIPLE-CONTACT VAPORIZATION TEST
P = 2535 PSIA T = 180 °F

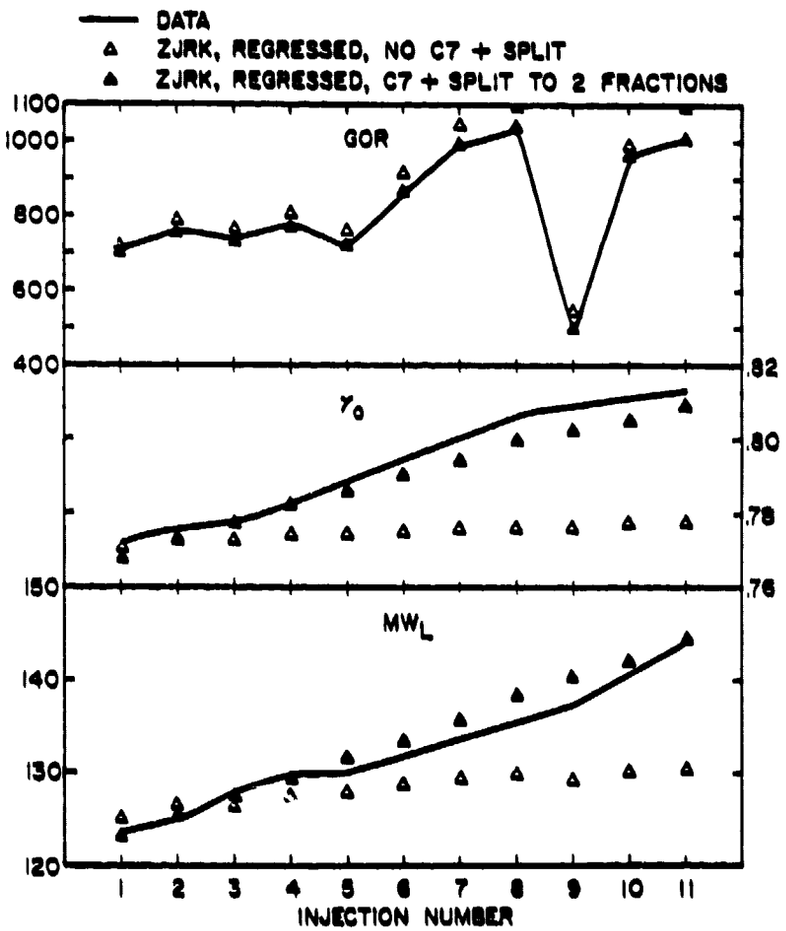

FIGURE 11
OIL 2 DIFFERENTIAL EXPANSION

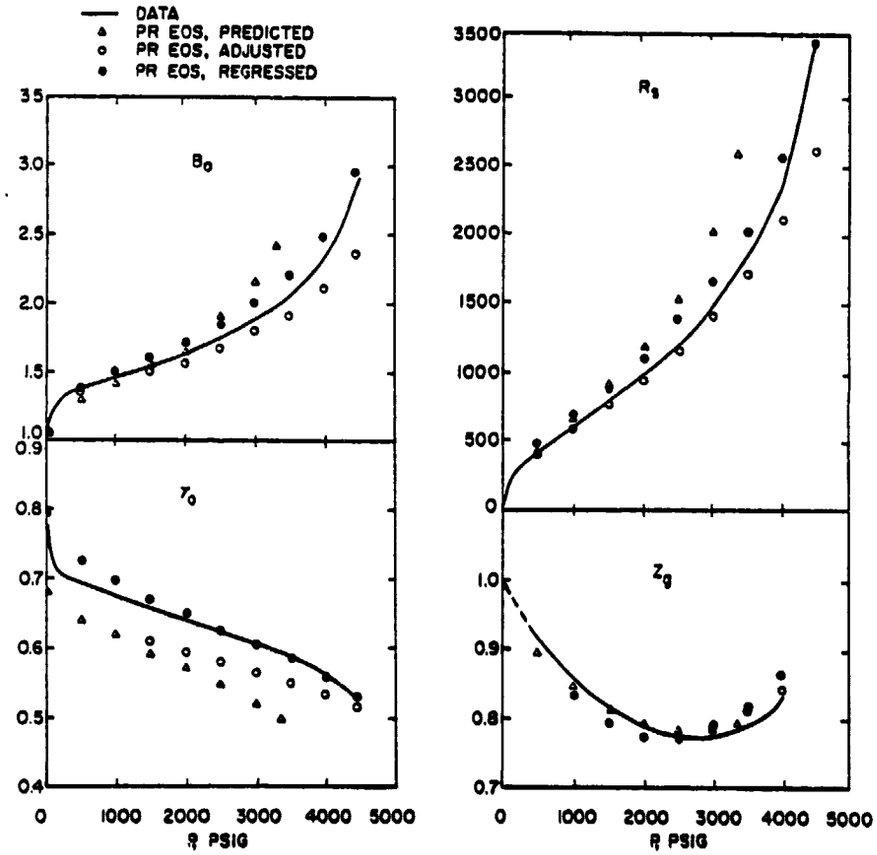

FIGURE 12
OIL 2 DIFFERENTIAL EXPANSION

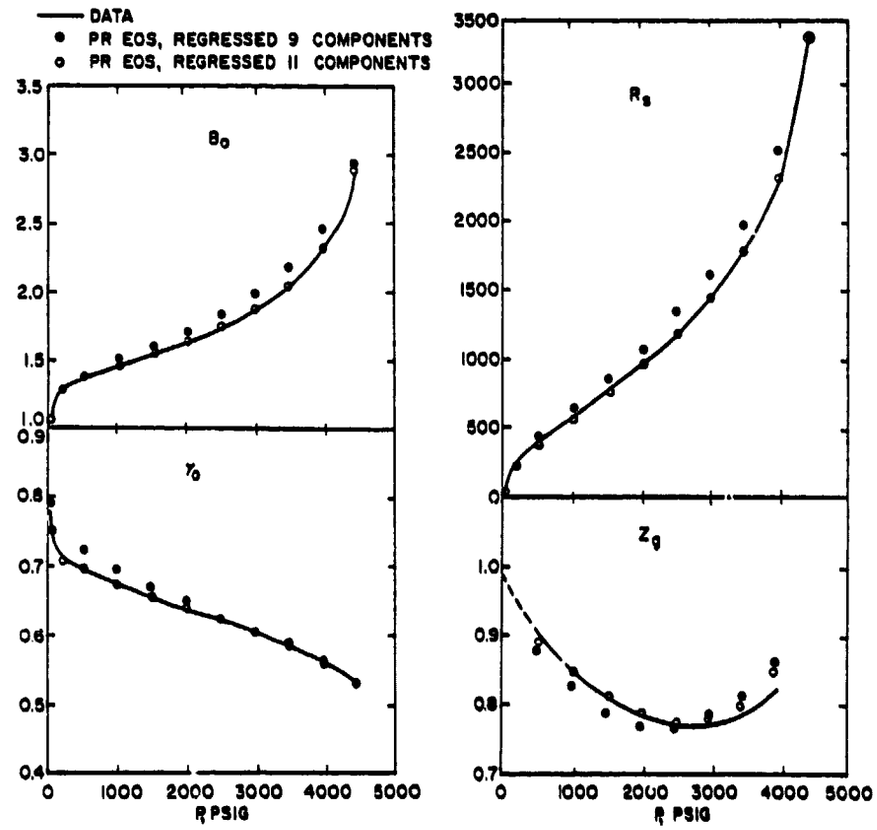

FIGURE 13

EFFECT OF TEMPERATURE ON SATURATION PRESSURE

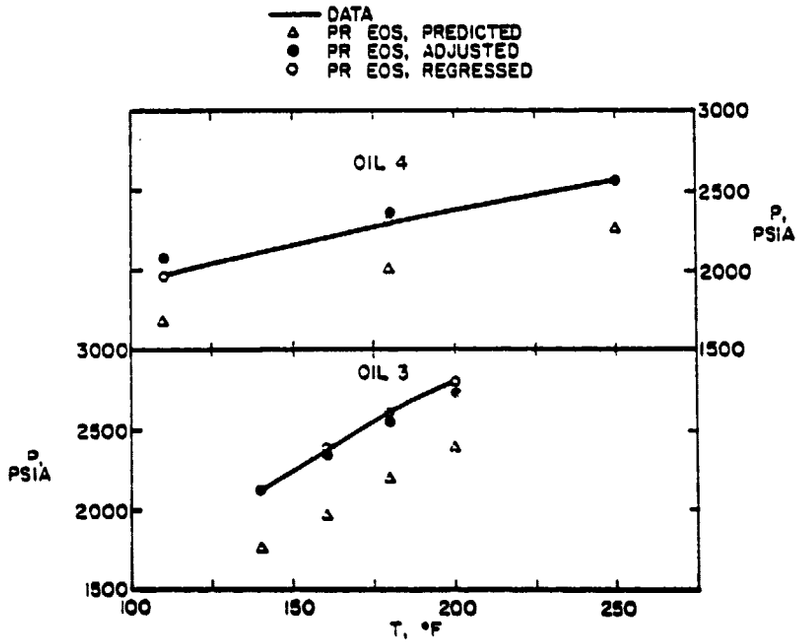

FIGURE 14

OIL 3 CONSTANT COMPOSITION EXPANSION

T = 180 °F

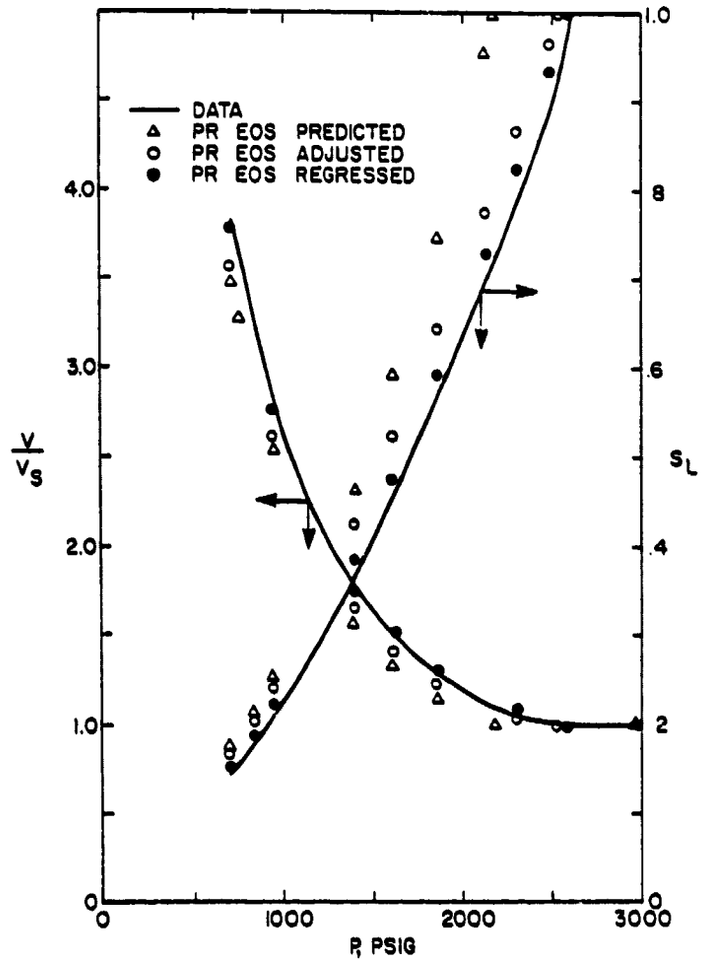

FIGURE 15

OIL 4 DIFFERENTIAL EXPANSION

T = 110 °F

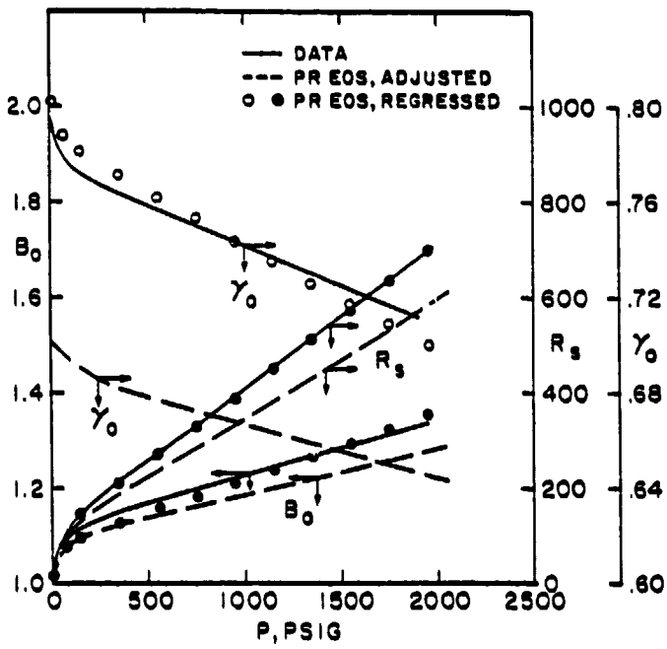

FIGURE 16

CONSTANT COMPOSITION EXPANSION OF OIL 5 ASSOCIATED GAS

T = 201 °F

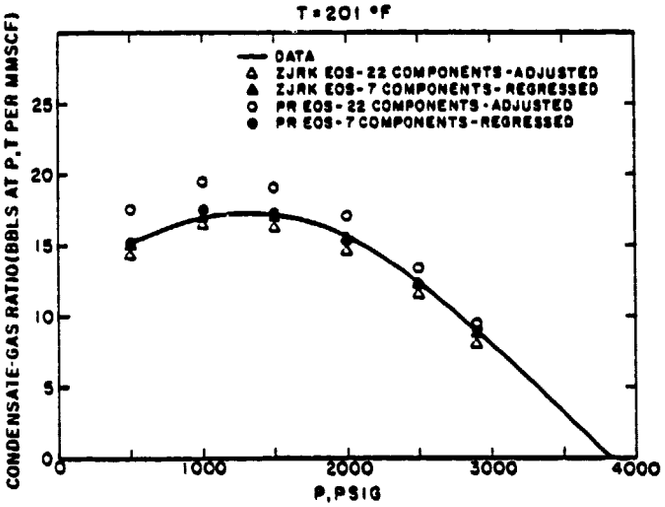

FIGURE 17

GRAVITY OF SEPARATOR LIQUID, CCE OF ASSOCIATED GAS FROM OIL 5

T = 201 °F

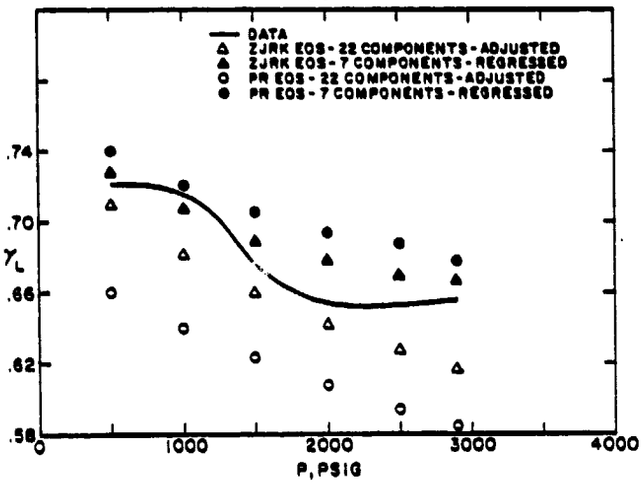

FIGURE 18

OIL 6 DIFFERENTIAL EXPANSION

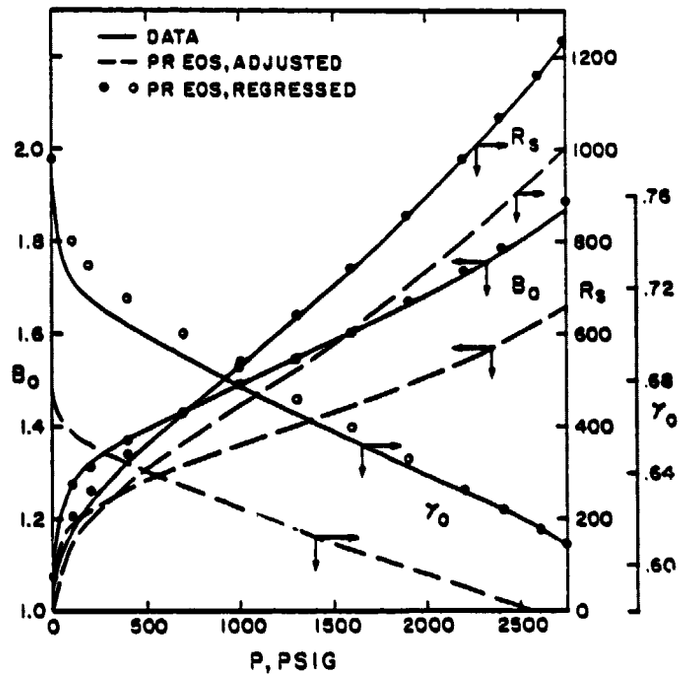

Errata (alteration) for purpose of review for SPE 11197

Oil 1

Oil 1, with composition given in Table 9, has a saturation pressure of 2535 psia at 180°F. This fluid was subjected to a multiple-contact vaporization test in which gas, with composition given in Table 13, was injected into the oil sample in a visual PVT cell at constant pressure and temperature in a series of steps. At each step, the fluids were allowed to reach an equilibrium. The gas was removed at constant pressure, and analyzed. The volume of oil was measured before the next gas injection took place. This process was continued for eleven injection steps. Measured data from this test are given in Table 13 and include the moles of gas injected and produced, the moles of liquid phase remaining in the cell, the composition of the gas at each injection step, and the composition and molecular weight of the residual oil after the last step of the test.

The PVT Program uses mass balance considerations to calculate additional data at each step, including oil and gas gravity and liquid phase molecular weight. The measured molecular weight of the C7+ of the gas at the different steps ranged from 105 to 110. The measured oil phase C7+ molecular weight for the reservoir fluid and last stage fluid were 225 and 258, respectively. The wide range of molecular weights of C7+ presented difficulties in matching the vaporization process with only one heavy fraction of molecular weight 225. The vaporized gas at each stage was too heavy, while the residual oil was too light.

A two-component split of the heavy fraction was defined with molecular weights 147.7 and 318.9 which gave mole fractions of .2646 and .2178 for components 9 and 10. This split system gave significantly better results than the non-split system as shown in Fig. 10. As Table 1 shows, the regressed, unsplit system gave an average deviation of about 3%. For the split system, the average deviation fell from about 6% after adjustment to .31% after regression, exhibiting an excellent match of the data. The regressed results shown in the figure were obtained using the PR EOS with regression on the multiple-contact vaporization data along with CCE data for the reservoir fluid and CCE data for the injection gas. Also shown in the figure are results obtained by adjusting only the binary in the PR EOS for the two-component split system. Results using the ZJRK EOS were very similar to the PR EOS results.

The additional definition of the C7+ allowed the vaporization process to be accounted for through stripping of the lighter of the two heavy fractions. Table 7 compares calculated and observed liquid and gas phase compositions at the last injection step. Further improvement in the match of these compositions might be obtained by extending the C7+ split. A first split fraction of molecular weight on the order of that of the removed gas, in the range 105-110, could allow both the gas gravity and the amount of C7+ in the gas phase to be matched.

TABLE 1
AVERAGE DEVIATIONS, SAMPLES 1-12 (%)

SAMPLE	N_c	J	PR EOS ADJ.	PR EOS REGR.	ZJRK EOS ADJ.	ZJRK EOS REGR.
GAS 1	9	17	32.50	1.50	31.10	1.47
GAS 2	9	57	29.49	6.20	28.42	6.08
GAS 2	11	57	12.48	5.01	9.20	4.05
GAS 3	10	13	50.83	1.79	44.35	1.83
GAS 4	12	11	48.00	0.67	59.40	1.02
GAS 5	9	42	17.07	6.73	15.61	7.16
GAS 5	10	42	13.09	6.01	9.75	5.52
OIL 1	9	57	12.12	2.88	7.28	2.77
OIL 1	10	57	6.42	.31	3.33	.27
OIL 2	9	79	10.25	4.68	7.25	5.66
OIL 2	11	79		2.71		
OIL 3	9	46	9.20	2.58	8.47	4.87
OIL 3	12	46	9.07	2.03	6.37	3.97
OIL 4	9	169	9.70	2.69	4.57	2.28
OIL 5	7	19	28.30	2.19	25.37	1.78
OIL 5	22	19	18.89	3.89	5.91	1.80
OIL 6	9	75	12.00	2.10	3.97	2.67
OIL 7	9	76	8.08	4.14	5.58	4.08
	AVERAGE		19.26	3.26	16.23	3.36

TABLE 4
FINAL VALUES OF REGRESSION VARIABLES

PR EOS

SAMPLE	N_c	$\bar{b}$	Ω^o_{a1}	Ω^o_{b1}	Ω^o_{a+}	Ω^o_{b+}	b_{1+}
GAS 1	9	.140	.420	.069	.430	.097	.408
GAS 2	9	.094	.708	.108	.264	.058	.200
GAS 2	11	.272	.600	.096	.391	.054	.037
GAS 3	10	.021	.494	.069	.278	.051	.156
GAS 4	12	.089[1]	.493	.073	.285	.042	.054[2]
GAS 5	9	.177	.593	.091	.342	.065	.295
GAS 5	10	.116	.577	.096	.342	.064	.191
OIL 1	9	.135	.501	.085	.763	.069	-.211
OIL 1	10	.056	.449	.082	.464[3]	.056[3]	-.186
OIL 2	11	.137	.323	.064	.539	.090	.178
OIL 3	9	.142	.438	.078	.529	.081	.084
OIL 3	12	.141	.436	.080	.420	.069	.072
OIL 4	9	.109	.554	.105	.411	.067	-.054
OIL 5	7	.092	.382	.050	.288	.066	.284
OIL 5	22	.253	.396	.067	.347	.044	.056[2]
OIL 6	9	.117	.313	.065	.478	.087	.157
OIL 7	9	.092	.482	.071	.371	.075	-.100

ZJRK EOS

SAMPLE	N_c	$\bar{b}$	Ω^o_{a1}	Ω^o_{b1}	Ω^o_{a+}	Ω^o_{b+}	b_{1+}
GAS 1	9	.101	.421	.077	.382	.105	.434
GAS 2	9	.038	.629	.110	.257	.069	.212
GAS 2	11	.299	.488	.103	.226	.045	.058
GAS 3	10	.079	.453	.085	.310	.058	-.030
GAS 4	12	.094[1]	.521	.095	.329	.056	0[2]
GAS 5	9	.143	.509	.090	.320	.077	.350
GAS 5	10	.148	.549	.103	.434	.075	-.017
OIL 1	9	.073	.445	.088	.798	.087	-.233
OIL 1	10	.043	.425	.087	.518[3]	.075[3]	-.104
OIL 2	11	.086	.344	.079	.500	.095	.151
OIL 3	9	.146	.361	.063	.616	.105	.150
OIL 3	12	.147	.382	.074	.610	.103	.134
OIL 4	9	.052	.475	.096	.504	.087	-.058
OIL 5	7	.039	.428	.051	.328	.085	.318
OIL 5	22	.182	.414	.083	.576	.082	0[2]
OIL 6	9	.061	.363	.082	.488	.098	.102
OIL 7	9	.017	.539	.092	.343	.071	-.050

(1) Methane Ω^o_b value

(2) This binary was fixed and not regressed upon

(3) Values for Ω^o_{a10}, Ω^o_{b10}. Regression also included Ω^o_{a9}, Ω^o_{b9}.

TABLE 7
FLUID COMPOSITIONS AT LAST INJECTION STEP FOR OIL 1

	LIQUID			GAS		
Component	Exp	PR no split	PR split	Exp	PR no split	PR split
CO2	.0060	.0037	.0048	.0085	.0086	.0086
N2	.0022	.0012	.0019	.0114	.0118	.0116
C1	.3480	.3829	.3425	.8776	.8887	.8800
C2	.0680	.0372	.0523	.0703	.0703	.0704
C3	.0279	.0141	.0217	.0165	.0163	.0165
C4	.0064	.0037	.0062	.0025	.0024	.0026
C5	.0051	.0013	.0031	.0009	.0006	.0008
C6	.0204	.0043	.0147	.0023	.0013	.0024
C7+	.5159	.5516	.5528	.0100	.0000	.0070

FIGURE 10

OIL I MULTIPLE CONTACT VAPORIZATION TEST

P=2535 PSIA T= 180°F

— DATA

● PR, REGRESSED, NO SPLIT

△ PR, ADJUSTED, SPLIT

▲ PR, REGRESSED, SPLIT